Aalto University
School of Engineering

School of Engineering

Department of Civil and Environmental Engineering

Daniil Iakovlev

Comparison of Barton-Bandis and Mohr-Coulomb models for use in discontinuity shear stability analysis

Supervisor	**Prof. Mikael Rinne**
Advisor	**M. Sc. Mikko Lamberg**

Master´s thesis which has been submitted for Master of Science degree.

At Espoo, 05.10.2015

Aalto University
School of Engineering

Aalto University, P.O. BOX 11000, 00076 AALTO
www.aalto.fi

Abstract of master's thesis

Author Daniil Iakovlev

Title of thesis Comparison of Barton-Bandis and Mohr-Coulomb models for use in discontinuity shear stability analysis

Degree programme Structural Engineering and Building Technology

Major/minor European Mining Course / Computer Science and Engineering **Code** R3008

Thesis supervisor Prof. Mikael Rinne

Thesis advisor(s) M. Sc. Mikko Lamberg

Date 05.10.2015 **Number of pages** iv + 62 **Language** English

Abstract

For mining and civil engineering projects rock slope stability is an essential part of safety and financial considerations. While large-scale stability can be simulated using rock mass properties, at smaller scale local variations in rock properties become significant and failure purely along discontinuities is possible. Wedging and rockfall are common occurrences at this scale. These are often prevented by bolting or shotcrete support. For temporary slopes such support measures can be costly, and an ability to simulate possible failures along discontinuity planes becomes useful for evaluation of support necessity. Traditionally the Mohr-Coulomb failure model has been used. However, a model has been developed specifically for discontinuity shear strength analysis. This Barton-Bandis model is based on basic friction of rock and joint roughness.

This study aims to compare the two models in practice both for accuracy and resources required. This is accomplished by carrying out a case study on the Siilinjärvi mine site rocks. Parameters for both models were collected with laboratory and in-situ tests. These included shear box, Schmidt hammer and tilt table tests as well as joint roughness profiling. The variability of these parameters was analysed and certain parameters were selected as the most appropriate for simulation. Several failure and non-failure cases were then simulated using these parameters to check their validity.

Parameters were easier to obtain for the Barton-Bandis model. Additionally, the variation in Barton-Bandis predictions for each sample was considerably smaller than the variation for Mohr-Coulomb predictions, and using the average of Mohr-Coulomb parameters would create a dangerously overconfident estimation of strength. Barton-Bandis results were easier to interpret. Parameters selected for simulation were preliminarily shown to be valid. It was found that joint continuity is a decisive factor for simulation even at small scale, and that assuming continuous joints can create disproportionately conservative strength estimates.

Keywords shear strength, discontinuity, joint, Barton-Bandis, joint roughness, joint matching, Siilinjärvi, open pit mine

Aalto-yliopisto
Insinööritieteiden
korkeakoulu

Aalto-yliopisto, PL 11000, 00076 AALTO
www.aalto.fi
Diplomityön tiivistelmä

Tekijä Daniil Iakovlev

Työn nimi Vertailu Barton-Bandis- ja Mohr-Coulomb-mallien käytöstä rakostabiliteetin analyysiin

Koulutusohjelma Rakenne- ja rakennustuotantotekniikan koulutusohjelma

Pää-/sivuaine European Mining Course / Tietotekniikka **Koodi** R3008

Työn valvoja Prof. Mikael Rinne

Työn ohjaaja(t) FM Mikko Lamberg

Päivämäärä 05.10.2015 **Sivumäärä** iv + 62 **Kieli** Englanti

Tiivistelmä

Kalliorakentamisen ja kaivosteollisuuden projekteissa kallioseinän stabiliteetti on olennainen osa rakennelman taloudellisuuden ja turvallisuuden tarkastelua. Suuren mittakaavan seinämästabiliteettia voidaan simuloida kivimassan ominaisuuksia hyödyntäen, kun taas pienemmällä mittakaavalla kiven ominaisuuksien paikallinen vaihtelu muuttuu ratkaisevaksi. Tällä mittakaavalla myös puhtaasti rakopintoja pitkin tapahtuvat sortumat ovat mahdollisia. Kiilasortumat ja kivien putoamiset ovat yleisiä ilmiöitä, jotka usein estetään pulttaamalla tai ruiskubetonoinnilla. Tilapäisien seinämien ja luiskien tapauksessa tällaiset tuentatoimet voivat olla kalliita, jolloin kyky simuloida rakopintoja pitkin tapahtuvia sortumia on hyödyksi tuentatarpeen arvioinnissa. Perinteisesti Mohr-Coulombin lujuusmallia on käytetty, mutta on kehitetty lujuusmalli myös nimenomaisesti raon leikkauslujuuden tarkasteluun. Tämä Barton-Bandis-malli perustuu kiven peruskitkaan sekä rakopinnan karkeuteen.

Tutkimuksen tavoitteena on vertailla näiden mallien tarkkuutta sekä niihin tarvittavia resursseja käytännössä. Vertaus tehtiin tapaustutkimuksella Siilinjärven kaivoksella. Molempien lujuusmallien parametrit kerättiin laboratorio- ja kenttäkokeilla. Kokeisiin sisältyi leikkausrasiakoe, Schmidtin vasarakoe sekä kallistuspöytäkokeet ja rakopintojen profiloinnit. Näiden parametrien vaihtelua analysoitiin ja edustavat parametrit valittiin simulointiin. Joitakin sortuneita ja sortumattomia kohtia simuloitiin parametrien soveltuvuuden tarkistamiseksi.

Parametrien hankinta oli helpompaa Barton-Bandis-mallille. Barton-Bandis-mallin näytekohtaisten lujuusennusteiden vaihtelu oli huomattavasti pienempää kuin Mohr-Coulomb-mallilla. Käyttämällä Mohr-Coulomb-mallin parametrien keskiarvoa saataisiin vaarallisen ylioptimistisia lujuusennusteita. Barton-Bandis-mallin tuloksia on näin ollen helpompi tulkita. Valittujen simulointiparametrien osoitettiin alustavasti olevan päteviä. Havaittiin, että rakojen jatkuvuus on ratkaiseva tekijä simuloinnissa myös pienessä mittakaavassa. Oletus rakojen täydellisestä jatkuvuudesta voi tuottaa suhteettoman konservatiivisia lujuusarvioita.

Avainsanat leikkauslujuus, rako, epäjatkuvuus, Barton-Bandis, rakokarkeus, rakoyhteensopivuus, Siilinjärvi, avolouhos

FOREWORD

This thesis study was commissioned and financed by Yara Finland for the Siilinjärvi open pit apatite mine. Work was carried out at the Aalto University rock mechanics laboratory and at the Rock and Tunnel Engineering department at Pöyry Finland. The study was advised by M.Sc. geologist Mikko Lamberg at Pöyry and supervised by Professor Mikael Rinne at Aalto. Other members of the advisory committee included Licentiates of Science Harri Kuula (Pöyry) and Sakari Mononen (Yara).

I would like to thank everyone involved in my studies and the making of this thesis. Professor Rinne introduced me to the European Mining Course and guided me during my Bachelor's and Master's studies. Sakari Mononen kindly invited me to study the Siilinjärvi mine site and mine geologist Mikko Suikkanen took time to help me with in-situ experiment arrangements. Pöyry and my manager Harri Kuula trusted me enough to provide the opportunity to carry out the study and write this thesis.

Doctor Juha Antikainen (Aalto) provided me with invaluable advice on rock mechanical aspects over the course of the study, while my advisor Mikko Lamberg was of great help in geological and mining aspects.

Another thank you goes out to peers and co-workers at both Pöyry and Aalto for providing pleasant and peaceful work environments and stimulating conversations. Especially I'd like to mention Lauri Uotinen at Aalto and Jouni Valli at Pöyry.

Finally, I'd like to thank my family for their support during the study and my life overall. To my parents over the years of support in my life and studies, and to my partner Kaisa Halmetoja for the mental support and shared worries.

TABLE OF CONTENTS

LIST OF SYMBOLS AND ABBREVIATIONS

SYMBOLS AND ABBREVIATIONS

a	maximum height of joint profile
BB	Barton-Bandis (model)
c, c_{peak}, c_{res}	cohesion (MC), peak and residual strength cohesion
d	diameter
JCS	joint compressive strength
JRC, JRC_0, JRC_n	joint roughness coefficient, sample JRC, scaled JRC (BB model)
L	length of joint profile
MC	Mohr-Coulomb (model)
SB	Shear box
UCS	unconfined compressive strength of rock

GREEK SYMBOLS

σ_c	see UCS
σ_{no}	normal stress
τ	shear strength
ϕ, ϕ_{peak}, ϕ_{res}	angle of friction (MC), peak and residual friction angles
ϕ_b	minimum angle of friction of flat surfaces (BB)
ϕ_r	friction angle of flat, sheared, weathered joint surfaces (BB)

1 INTRODUCTION

Stability of rock masses is an essential issue in many mining and civil engineering projects, as rock failures are a general safety issue. They are costly to clean up even when they do not happen to directly impact safety, and blocked passages incur losses due to the caused downtime. Often the rock is simulated as a single mass, only including jointing of the mass as a weakening parameter of the model. While this may work well for large-scale subjects, it is generally accepted that at small scale there are issues of joint stability and rockfall, shown by the tendency to attempt to prevent such events by the use of shotcrete and bolting.

In some cases, especially those of temporary slopes and tunnels, using such methods of strengthening the rock become costly to perform and certain risks are accepted instead. It is however possible to make a visual overview of an exposed rock surface to estimate the need for additional investigations, i.e. simulations of failure risks. Based on such simulations, risks can be reduced by either forcibly removing the risky area e.g. using blasting, or by using appropriate support methods. This study focuses on finding methods for obtaining parameters and simulating such small-scale failure risks.

1.1 STUDY OBJECTIVE

Two separate models of rock joint behaviour are compared: the Mohr-Coulomb model (MC) and the Barton-Bandis model (BB) using proposed methodologies. The comparison is carried out using a case study at the Siilinjärvi open pit mine, which is described in section 2. This includes obtaining critical parameters of each model using laboratory and in-situ tests and estimations based on earlier data. An attempt is then made to scale the obtained parameters empirically by simulating known failures.

Two main factors are considered when evaluating each model and method: the accuracy of obtained results and the amount of work required to obtain necessary parameters. Accuracy is evaluated using deviations of back-calculation predictions from actual failures. Work and resources here include various costs and availability of necessary equipment and expertise.

Based on this evaluation, a method for small-scale stability analysis at the case location is described and implemented. Preliminary parameter results for the studied case are presented and evaluated, with suggestions for future research.

Research questions

- What are the most practical rock mechanical parameters for small-scale stability analysis, at Siilinjärvi and in general?
- What are the main differences in using MC and BB models?
- What is the most practical way to collect data for bench failure simulations?
- Does the BB model create added value for short-term planning?

Methods

For each of the compared joint behaviour models, a set of suggested laboratory tests is performed on already available samples of Siilinjärvi glimmerite and diorite joints. These include shear box tests and tilt table tests for joint surfaces and drill cores in the laboratory. Additionally, Schmidt hammer tests and joint profiling are performed both in the laboratory and in-situ conditions.

Shear box test results are fitted to generate Mohr-Coulomb parameters. The other tests together with prior knowledge of the uniaxial compressive strength in different rock types are used to generate Barton-Bandis parameters. The obtained parameters are then used to simulate known

failures and non-failures at Siilinjärvi, and resulting safety factors are analysed for possible corrections of the parameters.

Based on the study, an evaluation of necessary resources and costs for each method is carried out. The more suitable model is selected based on correlation of simulations to failures and the aforementioned resource evaluation.

1.2 SHEAR BEHAVIOUR OF ROCK JOINTS AND TWO MODELS OF JOINT SHEAR STRENGTH

Rock failure is one of the most important research subjects in rock mechanics, and many failure criteria or models have been developed, the most used of which are the Mohr-Coulomb and Hoek-Brown failure criteria, often applied to rock mass. However, each failure model or criterion was developed from its own perspective, and due to the natural variability of rock and rock masses none of these is perfect for any circumstances; rather, it is up to the engineer to select the appropriate method for the circumstances and requirements of each case. (Ulusay & Hudson, 2012).

Fractures or discontinuities in rock play a significant role on rock mass stability and this is taken into account in used failure criteria – however mostly as a parameter of how fractured the rock mass is rather than behaviour of single discontinuities, as large-scale failures are almost invariably caused by a combined failure of the components of the blocky product of existing discontinuities. (Muralha, et al., 2013, p. 291; Bandis, et al., 1981, p. 15). This is, of course, an inevitable simplification, as it is nearly impossible to know the exact structure of discontinuities within a large rock mass.

At smaller scale, where discontinuities are continuous enough for failure to occur purely along them, it makes sense to simulate failure behaviour along the discontinuities, such as wedge failures (Figure 1-2). Other failure types typical for hard rock are also presented in Figure 1-2. Wedging and plane failures both represent sliding along a discontinuity surface, or possibly two in the case of a wedge. Toppling represents tensile failure in rock, usually due to steeply dipping discontinuities with no tensile strength. Circular failure is also possible in hard rock if the rock is fractured enough. More commonly circular failure occurs in soils and dumped rock with little or no cohesive strength between relatively small blocks or particles.

On the other hand, behaviour of jointed rock mass cannot be directly deduced from joint behaviour studies alone. For instance, it has been shown that closely jointed rock mass with smaller blocks is likely to have higher peak shear strength than one with larger blocks (Bandis, et al., 1981, p. 15).

Shear strength of discontinuities has several components (Figure 1-1). The base component is the basic frictional component, which represents a direct relationship between normal stress and shear strength based on frictional characteristics of the rock, weathered or not. On top of that any roughness, composed of geometrical variability of the joint and any asperities it has, creates extra shear resistance. It has however been shown that often the effect of the roughness component decreases as the joint length increases. This is partly due to the change of effective roughness with scale (see sample cuts 1-4 in Figure 1-1), and partly due to changes in intact asperity strength. Thus, a rougher joint can be expected to be affected by scale more than a smoother one. (Bandis, et al., 1981).

Though it is recognised that mechanical behaviour of rock joints alters as a function of scale, the size and direction of this effect is not consistent across studies. Many studies show negative scale effect, which means decreasing strength with increasing joint size, consistent with the idea of shear strength consisting residual friction plus a scale-dependent roughness component. Other studies show positive or no scale effect. Numerical experiments of sandstone joint models by Bahaaddini et al. (2014) support a negative scale effect, and note that failure modes at small and large scale are different. The authors also note that the growing peak shear displacement at longer joint lengths

implies that different asperity sizes control peak shear behaviour at different scales. For longer joints, the effective contact develops between asperities of flatter slopes and part of the shear strength comes from shearing off asperities, while for smaller samples shear behaviour is controlled by asperity wear. (Bahaaddini, et al., 2014).

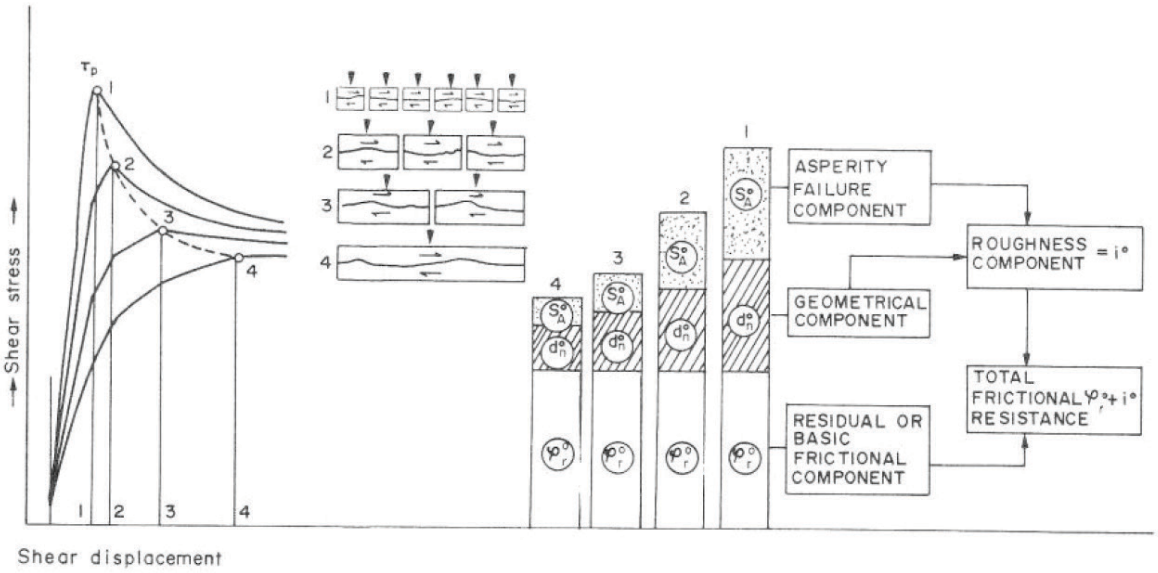

Figure 1-1: The two shear strength components of basic friction and joint roughness, and their length scale effect (Bandis, et al., 1981, p. 15) In general, longer joint samples lead to reduced shear strength. There is, however, no universal relationship for all joint types.

Overall the jury is still out on the defining factors of scale effect, however at least lower roughness can be assumed to diminish it, while correlation of roughness and undulation can determine the direction of the scale effect. For example, smooth joints with high undulation could be expected to have a positive scale effect, while rough planar joints would have a negative scale effect. Studies comparing on well matching joints (Kutter & Otto, 1990; Leal-Gomes, 2003) suggest a positive scale effect for fresh well-matched joints, possibly due to higher effective undulation in matching joints, as mismatched joints have virtually no effective undulation.

For the case of an ideal material, which would not break and have a very high elasticity modulus, the roughness would simply be added to the basic friction angle, creating a linear failure envelope. However, for less ideal materials the effect of the roughness component decreases as stress increases. This is due to asperity damage at high stresses. This effect is incorporated in rock failure behaviour models such as Hoek-Brown and Barton-Bandis models, but not in the Mohr-Coulomb fit. Issues occurring with linear fitting in MC are briefly described in section 4.1.

Discontinuity shear behaviour can be simulated by performing shear tests at different levels of normal stress, corresponding to the scenario of interest, and fitting the results to a model – most commonly the Mohr-Coulomb equation, described below. The empirical Barton-Bandis model, based on the rock's basic friction angle and the joint's roughness and compressive strength (Barton & Bandis, 1990), is also used for discontinuity stability analysis.

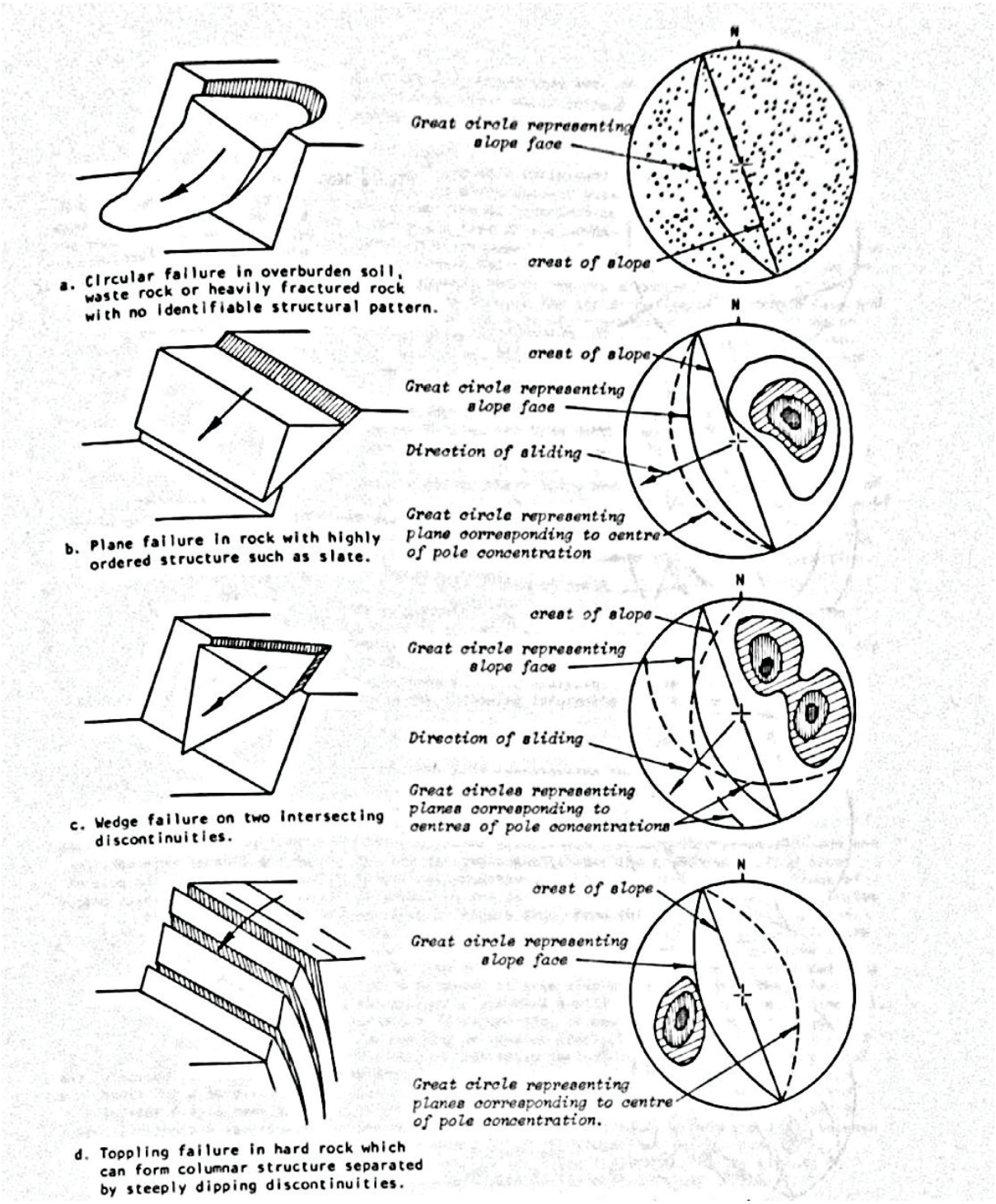

Figure 1-2: Slope failure types (Hoek & Bray, 1981, p. 57).

Mohr-Coulomb fit of shear tests

The Mohr-Coulomb equation (1.2-1) represents the shear failure envelope (Figure 1-3) of a material or, in this case, discontinuity surface: the maximum shear strength under various normal stress levels. It is, however, a linear fit, while the true shear failure envelope of discontinuity surfaces changes with increasing stress – at low normal stresses the shear strength is created by sliding along inclined roughness (teeth) of the discontinuity (Figure 1-4), while at higher stresses the teeth tend to break off resulting in lower shear strength, resulting in a curvilinear, rather than linear, shear failure or peak strength envelope (Hoek, 2006, p. 5; Barton, 1973, p. 287).

The cohesion and friction parameters are, in the case of non-cohesive materials, fitted calculation parameters of the equation and are not to be interpreted as e.g. actual cohesive strength of discontinuity surfaces. As Barton (1973, p. 303) puts it, “To rely on shear strength at zero normal stress is optimism taken to a dangerous extreme”. The parameters are thus dependent on and applicable for the normal stress range they are fitted for.

$$\tau = c + \sigma \, tan\varphi \qquad 1.2\text{-}1$$

(Hoek & Bray, 1981, p. 22)

where τ *is the material shear strength*
c *is the material cohesive strength*
φ *is the material friction angle*
($tan\varphi$ *being the coefficient of friction)*

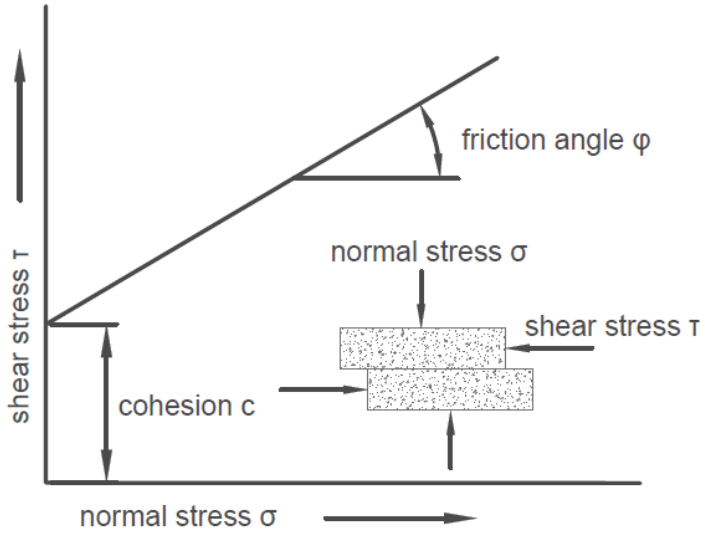

Figure 1-3: Mohr-Coulomb relationship between shear strength and normal stress acting on a surface (after Hoek & Bray, 1981, p. 22).

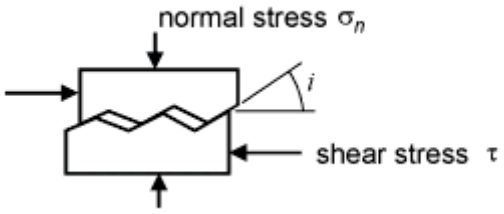

Figure 1-4: Sliding along discontinuity roughness (teeth) at low normal stresses (Hoek, 2006, p. 5).

Barton-Bandis model

The Barton-Bandis model for shear behaviour of rock joints is an empirical equation originally introduced in 1973 (Barton, 1973). The original equation (1.2-2) incorporates the effective normal stress, the joint roughness coefficient, joint compressive strength and the basic friction angle of rock. The basic angle of friction was later (Barton & Choubey, 1977) replaced with the residual angle of friction φ_r to accommodate weathering effects (equation 1.2-3).

$$\frac{\tau}{\sigma_n'} = \tan\left(JRC\ log_{10}(\frac{JCS}{\sigma_n'}) + \varphi_b\right) \qquad 1.2\text{-}2$$

(Barton, 1973, p. 326)

$$\tau = \sigma_n \tan\left(JRC\ log_{10}(\frac{JCS}{\sigma_n}) + \varphi_r\right) \qquad 1.2\text{-}3$$

(Barton & Choubey, 1977, p. 15)

where σ_n' *effective normal stress*
JRC joint roughness coefficient
JCS joint compressive strength
φ_b *basic friction angle of rock*
φ_r *residual friction angle of rock joint*

BB model parameters are directly linked to physical properties of the joints and can be understood intuitively. They are well introduced in Barton & Choubey's 1977 publication.

The basic (unweathered joints) or residual (weathered, filled, etc.) friction angle can be seen as the main parameter, as alone it represents the behaviour of planar joints where friction is the only force resisting shearing. The basic friction angle can be obtained by tilt testing sawn surfaces or drill cores, and the residual friction angle estimated by comparing the JCS and UCS of unweathered rock. These and other tests are described in Section 3 - Study methods .

The JRC parameter represents joint roughness; the rougher a joint, i.e. the more and steeper asperities it has, the more shear strength it has. Essentially the parameter represents all shear strength a joint has above basic or residual friction. Joint roughness can be evaluated visually by comparing to empirically obtained roughness profiles, or by back calculation of tilt test results of the joint of interest using the BB equation.

The third parameter, JCS, represents the compressive strength of the joint and is used together with normal stress to scale the effect of joint roughness. This scaling accounts for dilation and shearing of asperities, weakening the effect of JRC with higher normal stresses. The parameter is obtained using known UCS values of the rock in question and comparing Schmidt rebound hammer results on sawn, unweathered rock and on joint surfaces.

Both JCS and JRC scale with joint length as part of the roughness component. Empirical equations for scaling are provided by Barton & Bandis (1982, p. 750), however later studies (Castelli, et al., 2001; Ueng, et al., 2010) suggest these underestimate shear strength of longer discontinuities. In this study the JRC_0 and JCS_0 parameters are used for initial simulation input and scaling is carried out by back-calculation of known failures and non-failures.

1.3 SLOPE DESIGN

Both natural and man-made slopes of various sizes are a common occurrence in many civil and mining engineering projects, e.g. road embankments and open pit mine slopes. Slope design includes consideration of economic, environmental and safety factors, of which slope stability focuses heavily on the safety aspect. However, consideration of economic risk means that slope design is also affected by economic factors, i.e. costs of slope failure compared to costs and probability of stability, especially in mining projects.

In general, slope stability design consists of determining acceptable safety factors or probabilities for larger failures as well as rockfall, obtaining necessary geological and geotechnical information and simulating slopes using some method of analysis. A safety factor is defined as the ratio of maximum

forces resisting failure to forces driving failure. For more temporary slopes, using failure probabilities may be appropriate, as clean-up and other failure costs are considerably smaller than for e.g. a long-term civil engineering project, where reasonable certainty of long-term stability is preferred.

Acceptable safety factors are selected based on application, and vary from 1.25 to 2, usually being higher for permanent structures and lower for temporary slopes. These are based on observation and trial-and-error experiences (Wesseloo & Read, 2011, p. 223). Another option is to use acceptable failure probabilities in cost-benefit analysis: while a more stable slope is often more expensive to construct, failure near a ramp or road is far more costly than small-scale bench failure, and large-scale failures are of course more costly than small rockfalls. Probabilistic methods rely on input distributions of geotechnical parameters instead of single deterministic values, whereas deterministic safety factor methods are usually forced to use the most unfavourable parameter values when faced with uncertainty in data to avoid failures.

For temporary slopes it is important to consider the necessity of simulations in the first place. This consideration is based on experience, prior knowledge of the rock type properties and any other available information and observations. For some temporary slopes it may not make sense to gather new data or consider simulations due to low estimated risks and the temporary nature of the structure.

To simulate a slope the geotechnical properties of the slope material are necessary, as well as understanding of groundwater and climate conditions. Often literature values are used based on rock or soil type, as laboratory tests can be costly, time-consuming and inaccurate due to scale effects and other reasons. When past failure data is available, parameters can be back-calculated by simulating the failures. Geotechnical properties include material strength(s), weathering, and water permeability, as well as geological structure of the area, especially of discontinuity and weakness zones.

Armed with the necessary parameters, which can be expressed as deterministic values or probabilistic distributions, a slope is simulated and analysed for failure possibilities, usually for failure modes shown in Figure 1-2. For failures beyond the height of several meters, simulation is done as rock mass analysis. For smaller failure possibilities, where failures might occur purely along single discontinuities, discontinuity stability analysis may be used.

Limit equilibrium analysis can be used when only a safety factor needs to be obtained, and it is computationally light, though it requires simplification of geometrical and geological data. Numerical methods, on the other hand, are used to more fully simulate the response of rock mass to various conditions, such as faults and groundwater conditions. Due to limits on computational resources, many discontinuity properties are input as weakening parameters of the rock mass, and only critical discontinuities and weakness zones are simulated as separate zones. However, it has been noted that slope failures advance through internal discontinuities and weakness zones of a rock mass, and lately work has been done to incorporate such a failure method into slope stability simulation. (Suikkanen, 2014).

This study uses Swedge (Rocscience Inc., 2015) software for limit equilibrium analysis of wedge failures with two or three discontinuity surfaces and 3DEC (Itasca Consulting Group, Inc., 2013) numerical discrete element method for analysis of multiple block failure.

2 CASE: SÄRKIJÄRVI OPEN PIT

The Särkijärvi open pit, seen in Figure 2-1, is currently the main of two open pits at the Siilinjärvi phosphate mine site in Eastern Finland, owned and operated by Yara, a worldwide fertilizer and chemical supplier. Plants adjacent to the mine site refine the ore to produce fertilizers, phosphoric acids and apatite concentrate. Production at the mine site started in 1979, and life of mine plans reach until 2035. In 2013 an estimated total of 27 million tonnes of rock were mined at the site, including 11 million tonnes of ore. The current Särkijärvi pit is nearly three kilometres long in the north-south direction, 750 meters wide and has a depth of 250 meters. The current and designed pit limits are shown as a cross-section in Figure 2-2. (Yara, 2013; Lamberg, 2015).

Figure 2-1: View from south end of the pit. Photo provided by mine geologist Mikko Suikkanen (Yara).

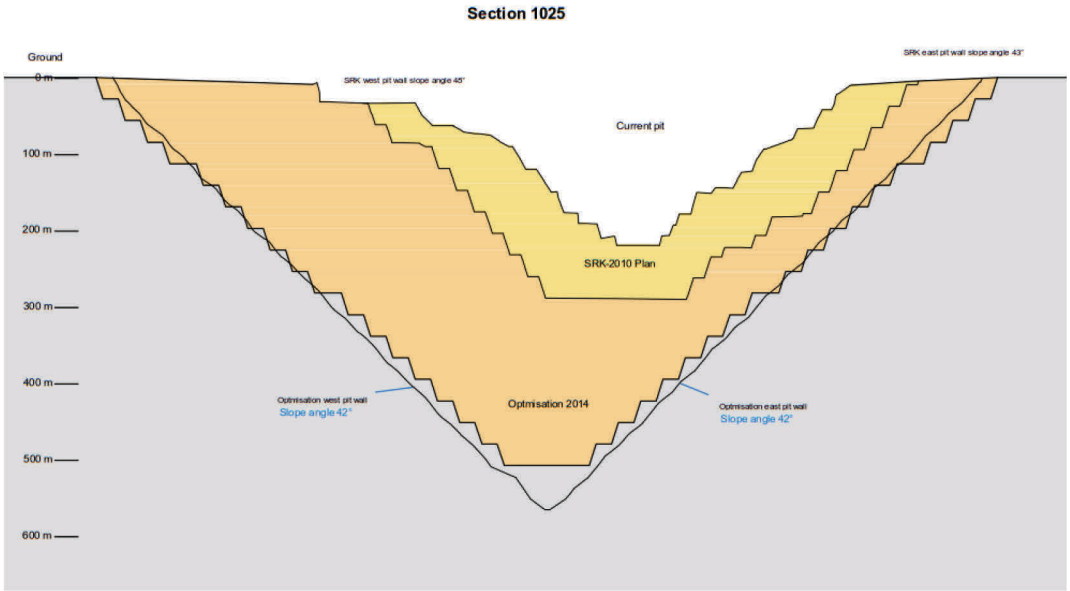

Figure 2-2: Current and designed pit limits (2010 and 2014 plans). Cross-section provided by Pöyry geologist Mikko Lamberg.

The mine site is surrounded by lakes and located close to the municipality of Siilinjärvi. The climate includes temperatures from several dozen degrees Celsius on both negative and positive sides of the

scale, and 24 to 50 mm of precipitation per month (Finnish Meteorological Institute, 2015), making ideal conditions for ice wedging in open pit walls in late autumn and early winter.

2.1 GEOLOGY

The main ore rock types at the Siilinjärvi carbonatite complex are glimmerite, carbonatite-glimmerite, silico-carbonatite and carbonatite. Waste rock mainly consists of outer fenite and inner northwest-southeast diabase veins and north-south diorite veins. Both ore and fenite dip about 85 degrees west. A geological map of the pit area is shown in Figure 2-3. The diabase and diorite veins are highly weathered at contact with other rocks, and their width varies between a few centimetres and sixty metres.

The latest southwest pushback has brought the pit into contact with diorite/tonalite areas, with new rock mechanical challenges due to planar and wedge failures in the pit walls. (Lamberg, 2015).

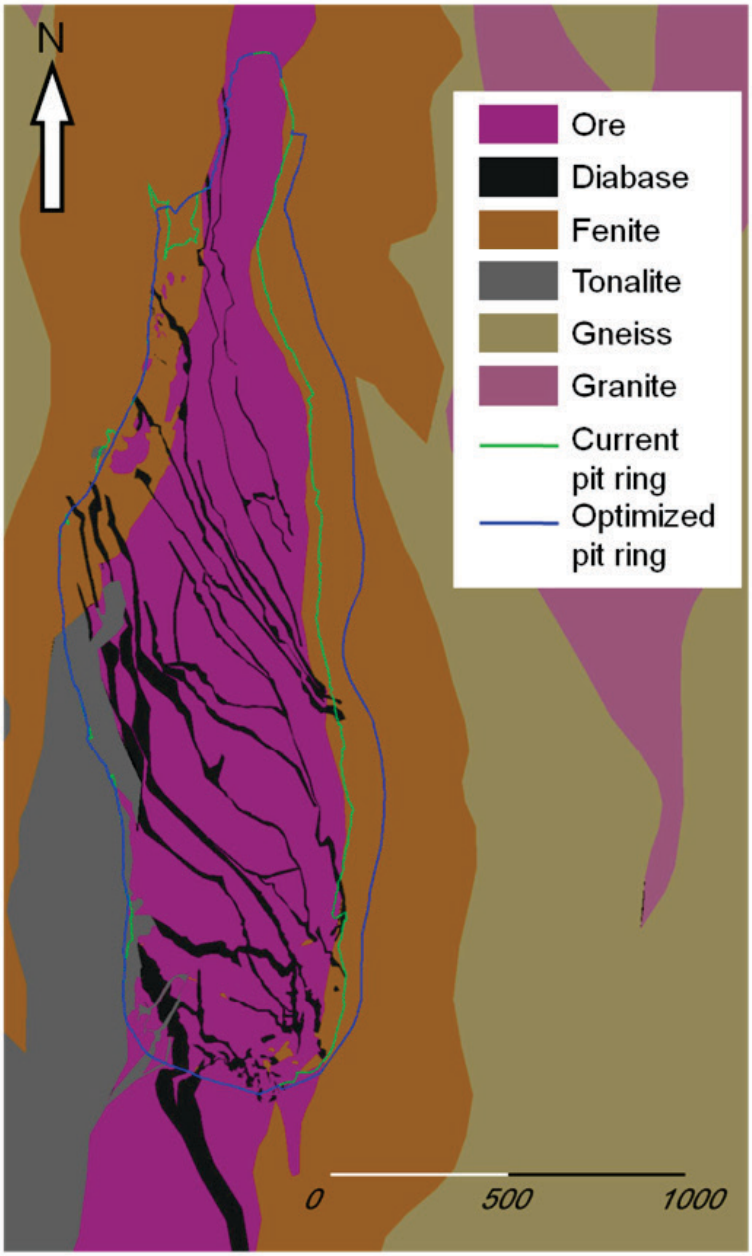

Figure 2-3: Geology of Särkijärvi area. Obtained by Jani Juvani (2013) from Yara geologist Pasi Heino.

2.2 ROCK MECHANICAL CONDITIONS

The rock mechanical properties of mine site rocks at Siilinjärvi is highly variable with different challenges presented. Failures at the site are dominated by jointing, mostly with plane or wedge sliding failures. Additionally, toppling failures occur at shear zone contact. Usually a shear zone area has collapsed partially along a joint plane, and rock mass failure occurs adjacent to jointing. This study focuses on the southwest diorite area and glimmerite ore, described below.

The outer waste rock (fenite and diorite) has two or more sets of highly planar joints, with joint continuity of several meters and sometimes up to 60 meters or higher and block sizes of several meters (Figure 2-4). There are also rougher joints of lower continuity; however, failures have not been observed originating along these joints.

Figure 2-4: Up to two benches of planar joint continuity in diorite. Photo provided by Pöyry geologist Mikko Lamberg.

The inner diabase (dolerite) waste rock veins have two to four joint sets and a smaller block size of 20 cm to 2 m. Besides local degradation of the surfaces due to small block size (Figure 2-5), contact between diabase veins and ore also has adverse frictional characteristics. Another challenge is brought by shear zones with variable, but low frictional characteristics (Figure 2-6).

Figure 2-5: Heavily jointed and blocky diabase waste rock (above) and undulating chlorite joint surface in ore. Photo provided by Pöyry geologist Mikko Lamberg.

The ore has smooth slickensided joints with chlorite filling and continuity of bench (height of 28 m) or even multi-bench size (Figure 2-5, Figure 2-7). When on the surface of joints the chlorite is hard and has very low friction. Besides being slickensided, the ore rock has a lower basic friction then the waste rock, and the chlorite filling lowers it even further. Unlike the waste rock, these joints undulate strongly, giving them at least some strength. The block size is also large, with blocks the size of a pick-up truck reported after failures.

Figure 2-6: A typical toppling failure in the shear zone. Here rock mass failure is observed. Note the small block size mixed with gravel and smaller grains.

Figure 2-7: Undulating joint surfaces in the orebody. (Nick Barton & Associates, 2014).

2.3 SLOPE DESIGN METHODS

The Särkijärvi final open pit design is based on ore reserve estimations and rock mechanical considerations. Here the scale and unknown specifics of rock mechanical conditions force the designers to work using rock mass behaviour models. The used rock mass properties, final depth and target safety factor are decisive in selecting the overall slope angle.

The bench height is mostly determined by limitations of drilling and loading equipment. Another factor is the minimal bench width together with the selected overall slope angle. The latest design (Figure 2-8) has kept an earlier design bench height of 28 meters, mined in two 14 meter parts, and widened the safety berm to 17 meters due to a lowered overall slope angle and experience with rockfall not being stopped at the first bench it encounters.

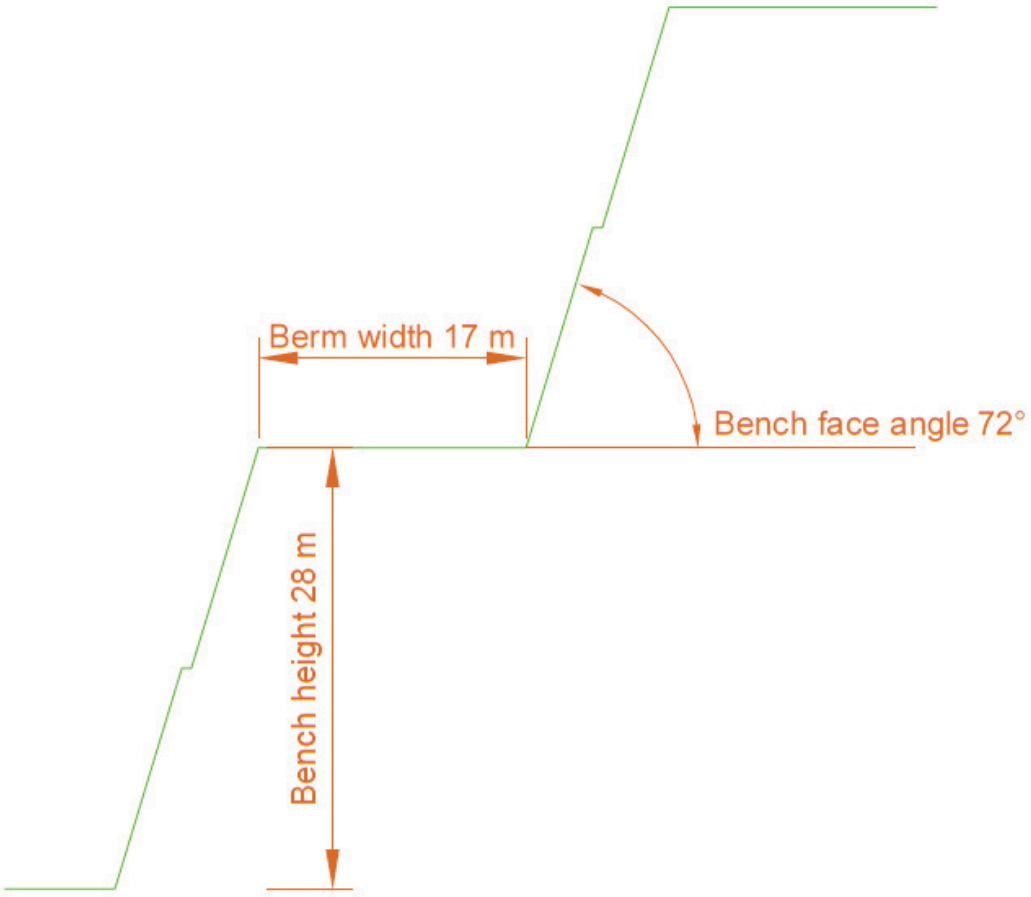

Figure 2-8: Section of current general bench design at Siilinjärvi. Ramps are 40 meters wide.

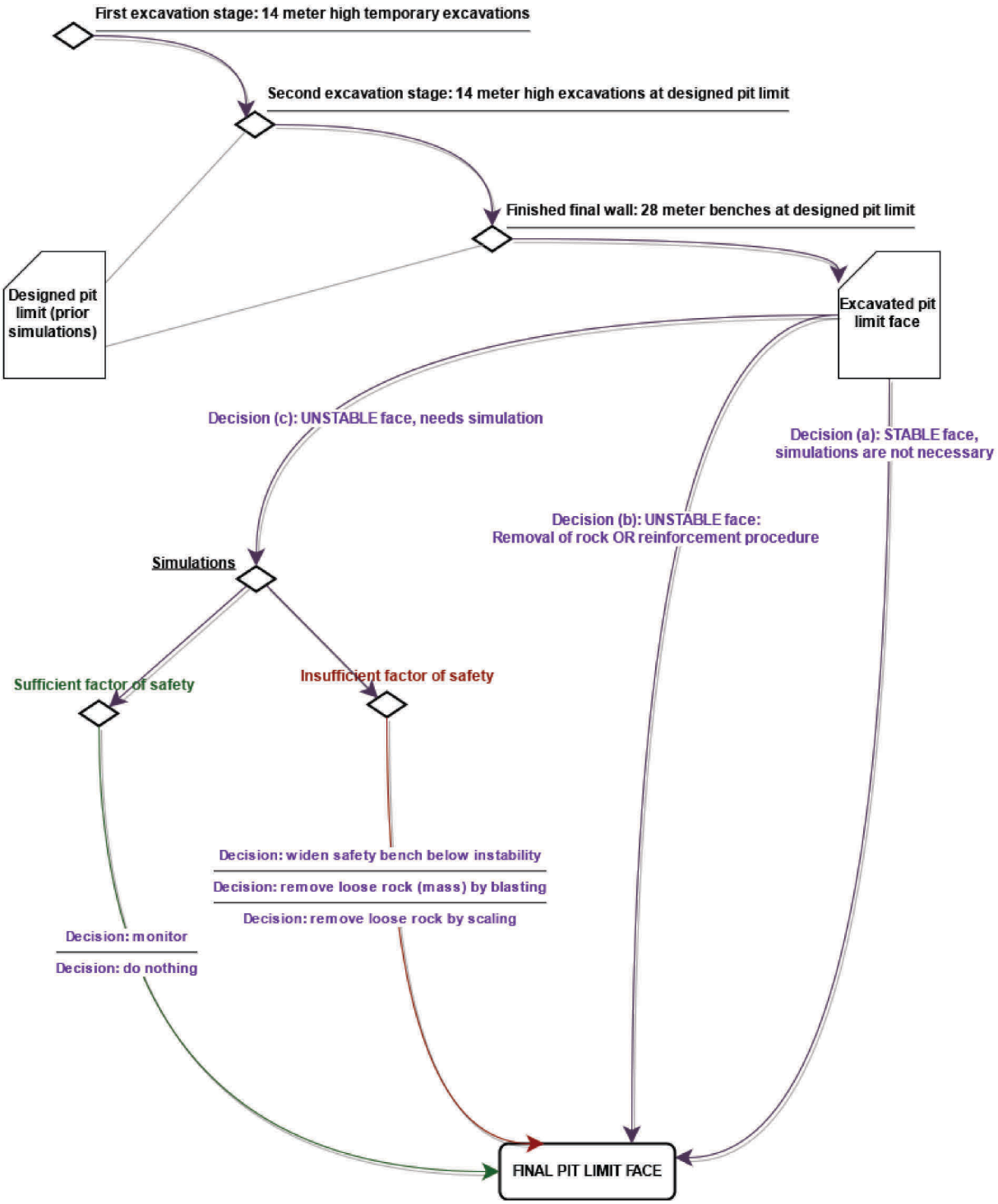

Figure 2-9: Slope stability design at Siilinjärvi. The second and third excavation stages use pre-split blasting, to create more even pit limit faces. Pre-split blasting is not used for temporary faces.

Rock mechanical simulations are done for the designed pit limit. When a final pit wall is exposed, the designers make an intuitive judgement on possible failure risks such as adverse jointing or clearly loose blocks. If these are found, they are then simulated, and if the simulation generates a safety factor deemed too low one or more of the methods in Figure 2-9 is applied. Often a safety factor limit of 1.5 is used.

The sensitivity of judging an area as possibly unstable is higher close to the current and designed ramps. Any wall above is under closer scrutiny due to risks of rockfall, and the wall immediately below the ramp due to risks of slips and ramp collapses in case of instability (see Figure 2-10).

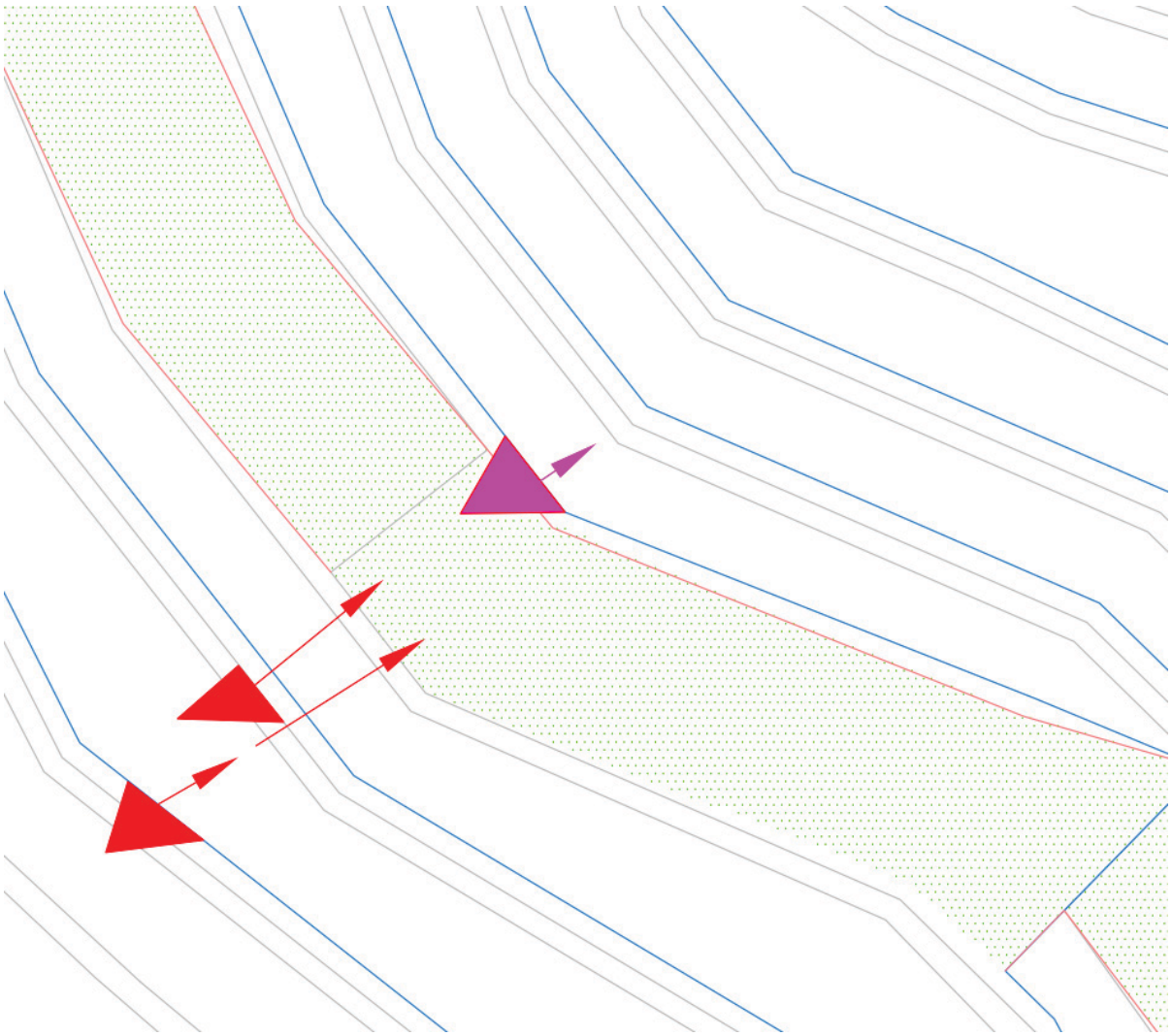

Figure 2-10: Risks of rockfall on ramp (shaded in green) from above (red) and slippage of rock immediately below (magenta) the ramp. Each blue line represents the foot of a 28 m high bench.

(Lamberg, 2015).

3 STUDY METHODS

Various laboratory tests were carried out to determine parameters for both the Mohr-Coulomb and the Barton-Bandis models. These are partly based on recommendations received from Nick Barton in a report on Siilinjärvi (Nick Barton & Associates, 2014), see Figure 3-1. The tests are described below and were carried out in the order they are introduced, except for the core tilt tests as they are carried out on completely separate samples which are not tested otherwise.

The parameters obtained from these models were used as initial parameters for simulations of rock failures. These simulations are meant for validation of the obtained parameters and comparison of results generated by the MC and BB models. The simulation process is described in section 3.2.

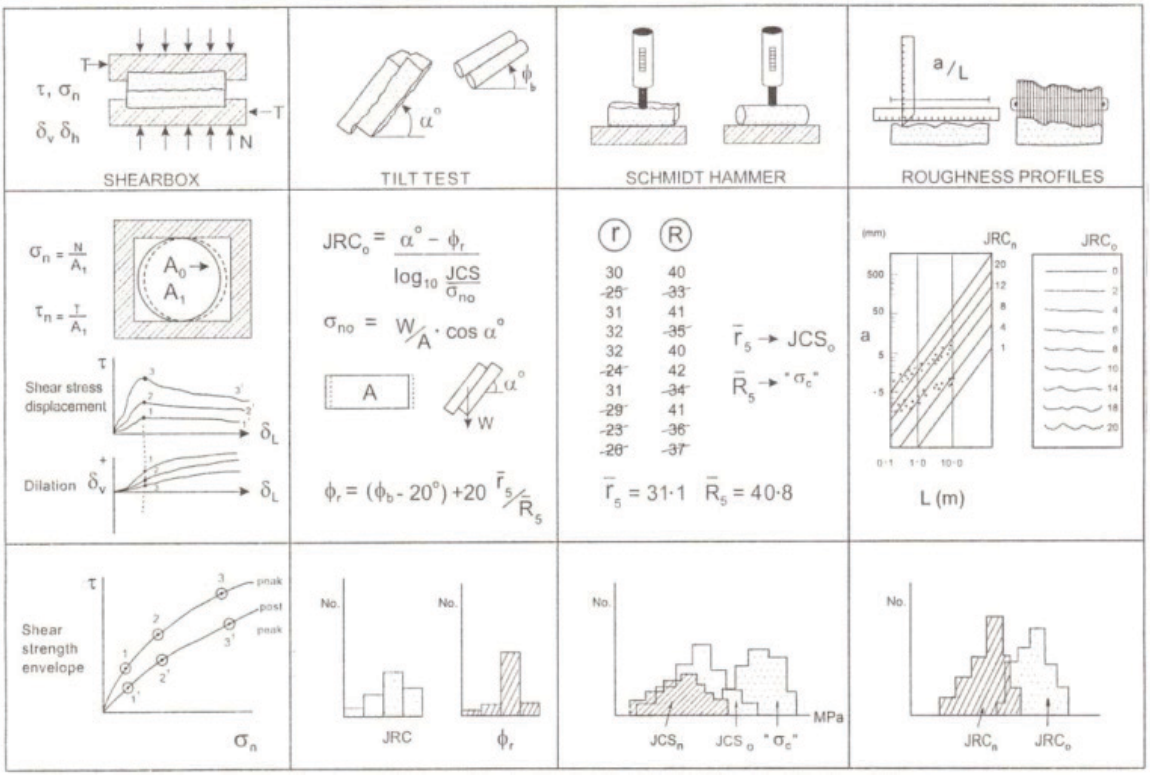

Figure 3-1: Tests recommended by Barton (Barton, 1999, p. 1661; Nick Barton & Associates, 2014).

Descriptions of the samples used in the study were recorded, including rock type, visual properties of the rock and joint, and any alteration of the rock, especially joint filling. The sample type (e.g. core, field block, or collapse block), climate conditions, excavation type and moisture content are also included in the descriptions. These can be provided upon request.

3.1 LABORATORY AND FIELD TESTS

Prior known results, test methods used in the study and sampling handling procedures are described below.

Prior results

There is a very limited amount of laboratory tests of joints carried out on Siilinjärvi samples. A report (Kauppinen, 1989) shows that shear box tests for diabase and ore were carried out at normal pressures of 0.14-1.7 MPa, resulting in an MC fit of τ = 0.110-0.370 MPa + σ_n tan 37-42° for ore and τ = 0.220-0.420 MPa + σ_n tan 26-45° for diabase. The report does not state whether the tests were carried out in multiple or single stages, but considering that only six samples were used multi-stage

testing (Figure 3-2), is likely. Multi-stage testing can be done either without resetting the sample movement, instead changing the normal load after a certain shear length (Figure 3-2 a), or with resetting the movement between changes in normal load (Figure 3-2 b). Correspondingly, in single stage testing a single sample is tested under a single normal load, and other samples from the same testing horizon are tested at other normal load levels. This requires considerably more samples to achieve the same amount of data.

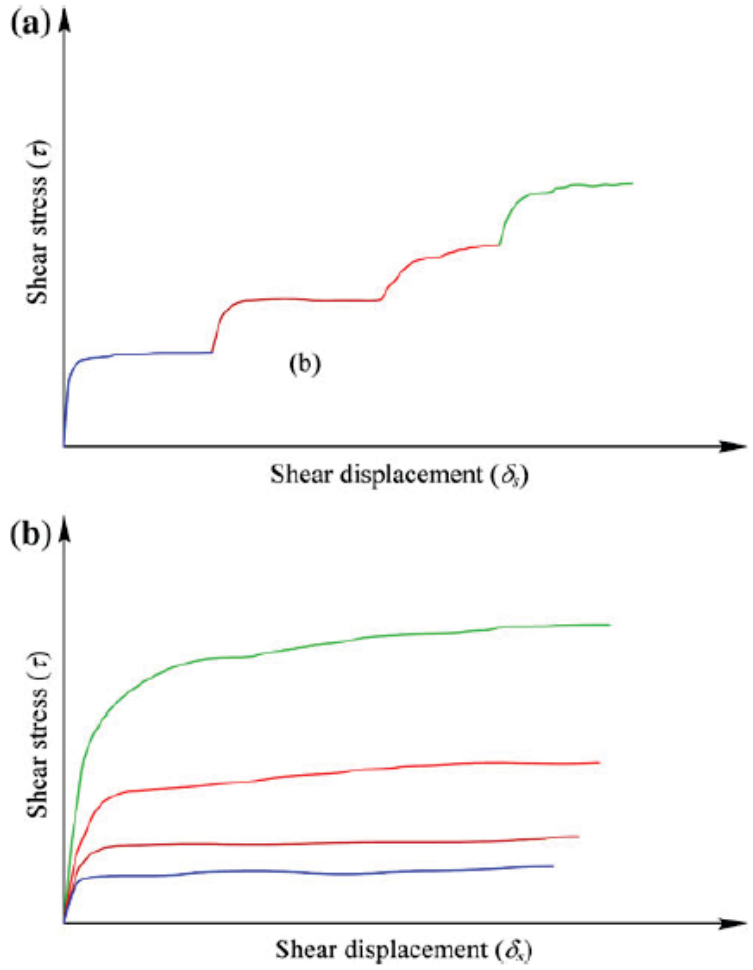

Figure 3-2: stress-displacement curves for multi-stage testing with (b) or without (a) resetting the sample movement. (Muralha, et al., 2013).

Results of UCS tests of the rock types at Siilinjärvi were provided by Pöyry (Table 1).

Table 1: Unconfined compressive strength (CS) values of Siilinjärvi rocks. Data provided by Pöyry (Lamberg, 2015).

Rock type	Avg CS	StDev of CS	Sample count	Avg-StDev
CRB-GL	*56.0*	*27.7*	*17*	*28.3*
Carbonatite CRB	*68.9*	*40.3*	*9*	*28.6*
Diabase DB	*207.6*	*51.7*	*6*	*155.9*
Diorite DR	*247.8*	*30.7*	*5*	*217.1*
Fenite FEN	*151.2*	*60.0*	*7*	*91.3*
Glimmerite GL	*53.7*	*25.6*	*23*	*28.1*
SCRB	*51.1*	*60.0*	*2*	*-9.0*

Determination of JRC_0 and JRC_n using the Barton comb profilometer

The joint roughness coefficient (JRC) was determined using a brush gage profilometer (Figure 3-3), also known as a Barton comb. Two approaches were used, both in accordance with Barton's (2014, pp. 31-37) recommendations.

For both approaches, the profilometer (maximum length of 250 mm) is pressed against the joint surface, with two to three measurements in the planned direction of testing and two-three measurements perpendicular to it. The first, subjective, approach is carried out by comparing the generated profile to the reference joint profiles provided by Barton (see Figure 3-4, left, and Figure 3-5) and given a roughness profile number, then converted to JRC_0.

The profile length L and maximum amplitude a are also measured for the second approach (Figure 3-4, right). Here JRC_n is determined by converting the a/L measurement using Barton's log-log scale sheet (Figure 3-6). In this study any profiling length of less than 100 mm is treated as 100 mm to avoid overestimation. JRC_n is then converted to the JRC_0 length (100 mm) by solving the empirical equation 3.1-1 numerically for JRC_0. For further purposes average JRC values in each direction and for each approach are used.

$$JRC_n = JRC_0 \left(\frac{L_n}{L_0}\right)^{-0.02JRC_n} \qquad 3.1\text{-}1$$

(Barton & Bandis, 1982, p. 750)

where

JRC_n	*JRC for non-standard length*
JRC_0	*JRC for standard length*
L_n	*Non-standard length*
L_0	*Standard sample length of 0.1 m*

Figure 3-3: Profilometer.

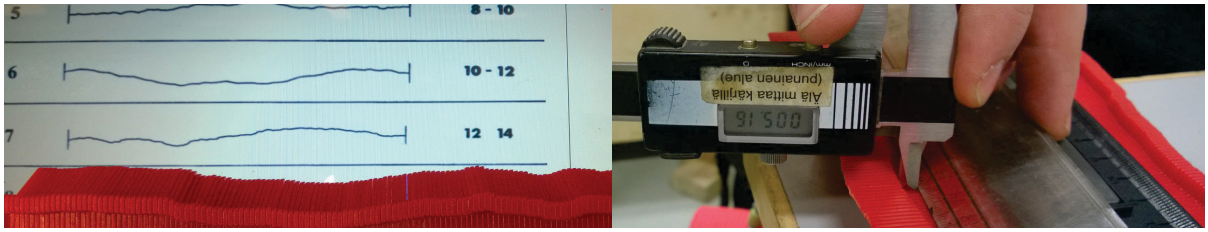

Figure 3-4: Profile comparisons (left) and height measurements (right). When comparing profiles it is important that the scale of the reference profile on screen or paper is correct.

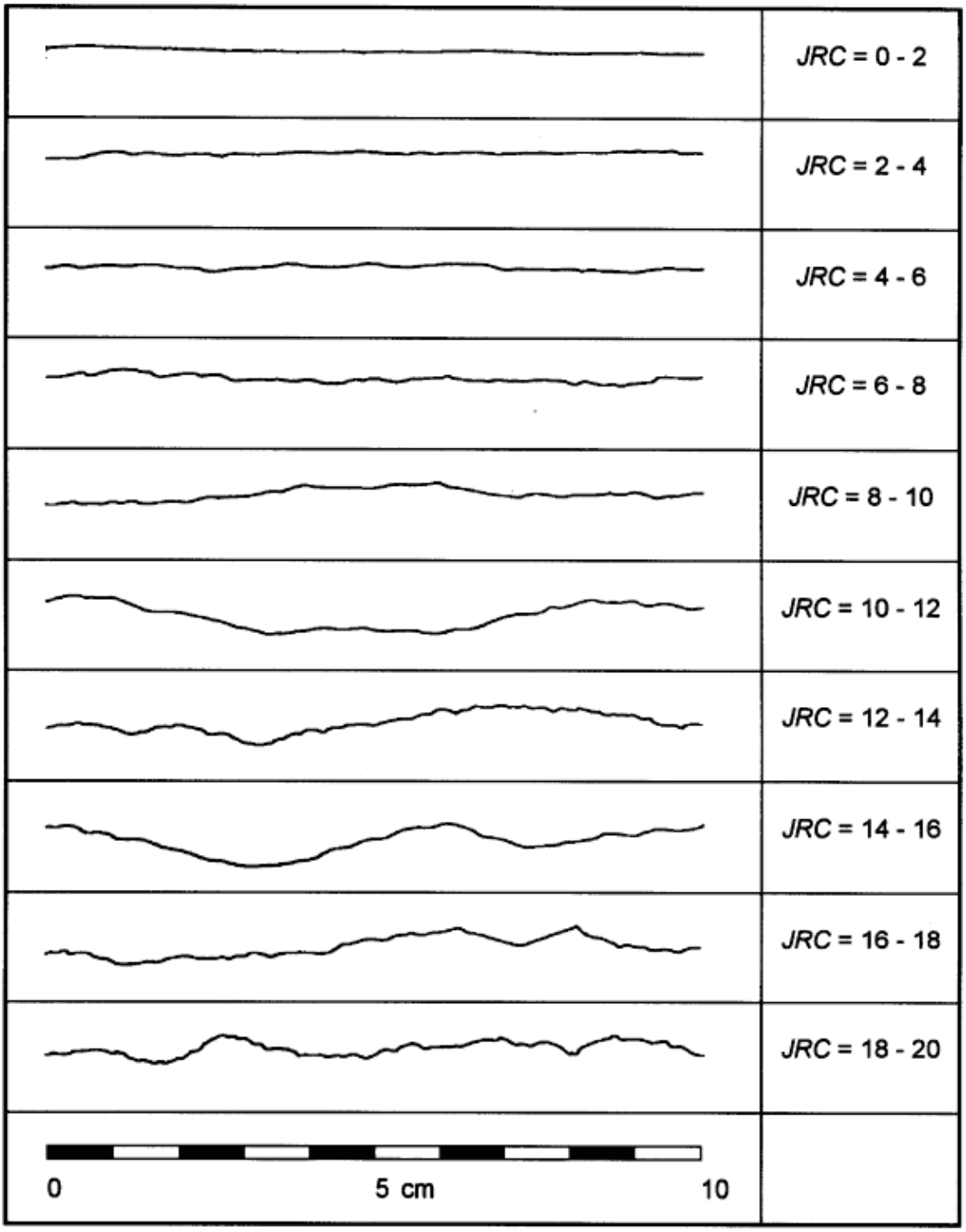

Figure 3-5: Roughness profiles (Hoek, 2006, p. 7; after Barton & Choubey, 1977).

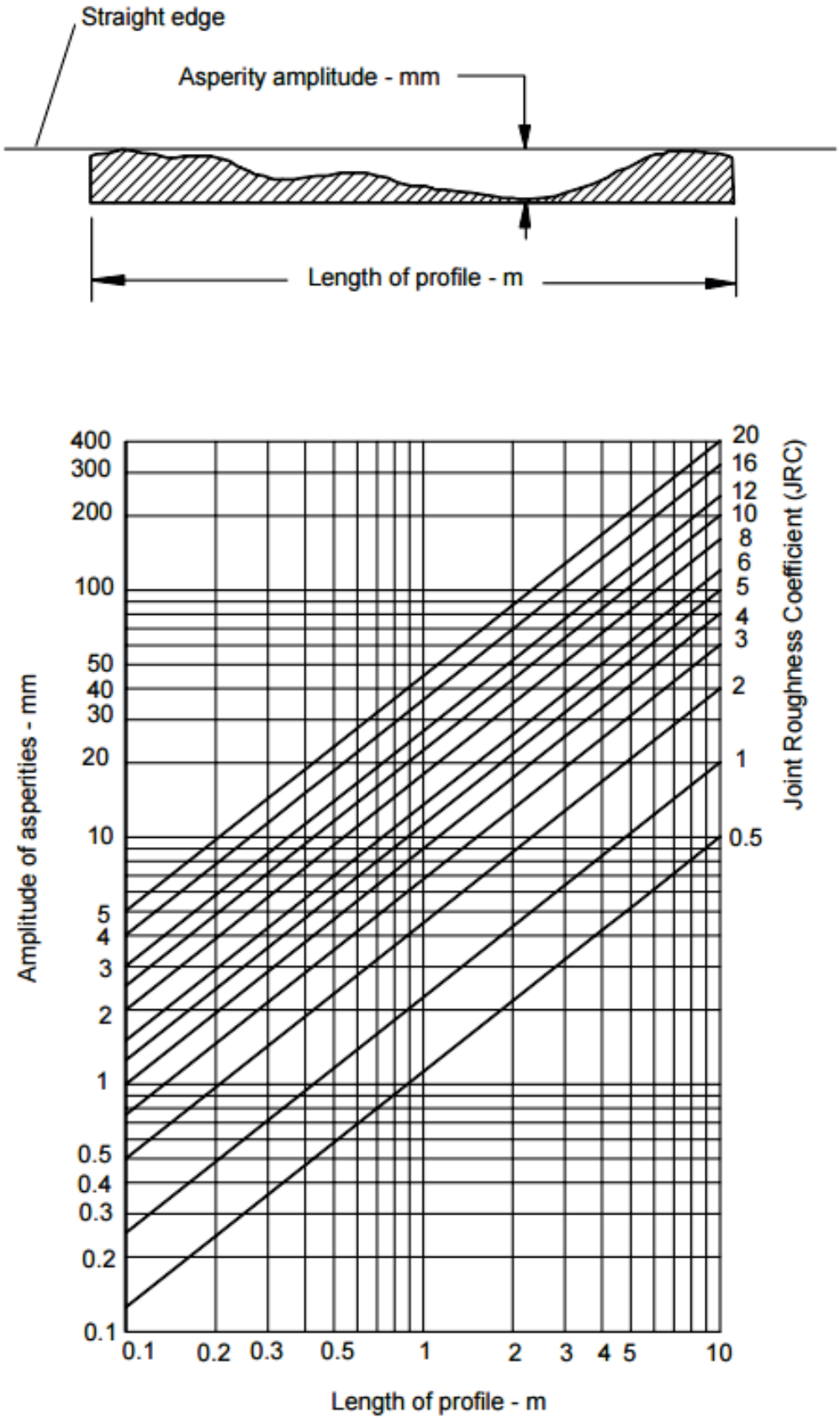

Figure 3-6: JRC estimation log-log sheet (Hoek, 2006; after Barton, 1981).
Alternatively, the equation $JRC = \frac{a}{2.2 \cdot L^{0.95}}$ *can be used, which is approximated from the graph.*

Essentially the same process was used to determine in-situ JRC_0 at the pit (Figure 3-7). Here, the full length (250 mm) of the comb could be used, giving more readily comparable results.

Figure 3-7: In-situ profiling.

Joint surface tilt tests for determination of JRC_0

Joint surface tilt tests are used to determine JRC_0 experimentally instead of by profiling. Additionally results are used as an extra data point to aid in determining MC parameters.

The samples are sawn to create simplified geometries for tilt testing. Sawing is described on more detail at the end of this section. As tilt tests of joint surfaces are currently recommended to be carried out at matrix saturation (Nick Barton & Associates, 2014, p. 36), the samples are then submerged in water for twenty-four hours or longer prior to testing. A possibility of damage to any possible joint filling exists during both processes of sawing and submerging in water. This possibility needs to be considered in later interpretations.

The tilt tests are carried out using a motorized tilt table (Figure 3-8), using a maximum speed of 0.25 degrees per second in accordance with Ruiz & Li (2014). One tilt test is carried out in the direction of shear box testing, and one in the opposite direction. JRC is then calculated using equation 3.1-2.

$$JRC = \frac{\alpha - \varphi_r}{log10(^{JCS}/_{\sigma_n})} \qquad 3.1\text{-}2$$

where α is the tilt angle at sliding

Adapted from (Barton & Choubey, 1977).

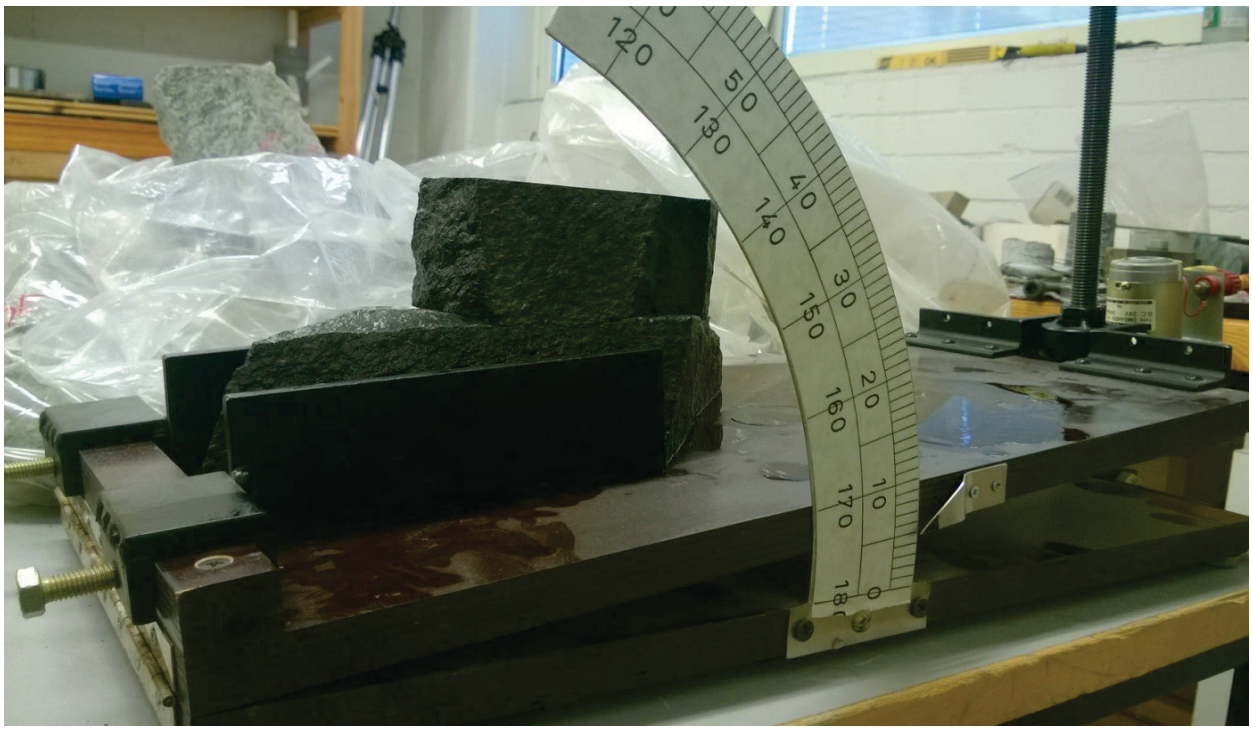

Figure 3-8: Tilt table.

Initial tests with diorite samples failed to produce a joint failure as the table could not rise high enough. The table was then pre-tilted to create a high enough maximum angle α to create a sliding failure in all tested samples. Samples were weighted and their total surface contact areas in plane projection were calculated prior to testing.

Tilt tests of core surfaces

A three-core tilt test was carried out to determine the basic friction angle of diorite and glimmerite. Ruiz & Li's (2014) description of the procedure and proposed correction formula (equation 3.1-3) was used to obtain the results. Each core compilation was tested several times, systematically rotating the core(s) between tests. The lowest result was selected for use to limit any geometrical effect of drill ridges.

$$\varphi_b = \tan^{-1}(\tan\beta \cdot 0.866) \qquad 3.1\text{-}3$$

where β is the tilt angle

The current recommendation is to use the two core tilt method due to a possible wedging effect if the two lower cores become separated (Barton, 2013; Barton, 2015). This effect was prevented by preventing the movement of the two lower cores (Figure 3-9) and a comparison of the two and three core method carried out by Ruiz & Li (2014) shows that the methods produce similar results. Core assembly for the three core test is shown in Figure 3-10.

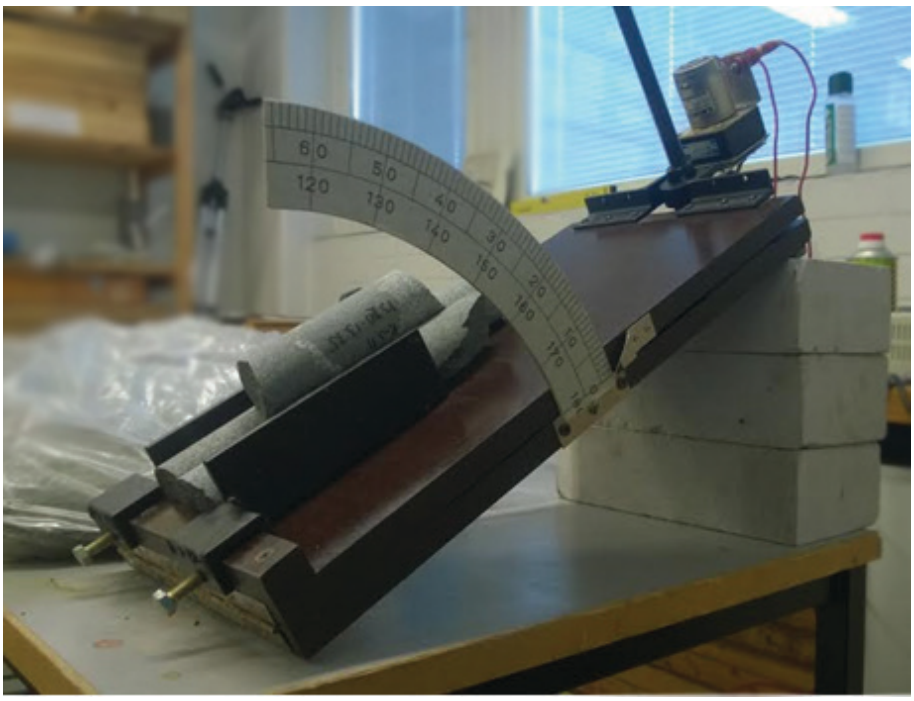

Figure 3-9: Three core tilt test setup.

Figure 3-10: Sample core assembly for the three core tilt test. Photo courtesy of Laura Tolvanen / Posiva.

Schmidt hammer tests

A Schmidt rebound hammer (Figure 3-11 and Figure 3-12) consists of a spring-loaded mass, which is released against the tested surface, and the rebound distance of the mass is recorded. The hammer was developed for determination of unconfined compressive strength (UCS) of concrete. In rock mechanical applications it is generally used for in-situ estimation of UCS of rock (Aydin, 2009, p. 627).

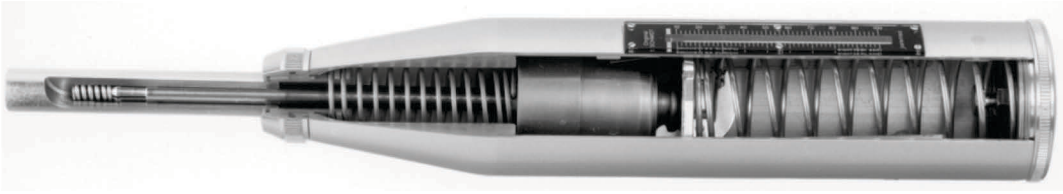

Figure 3-11: Schmidt hammer cross-section (Szilágyi, 2013).

Figure 3-12: Schmidt hammer use (Atlantic Supply, 2015).

In accordance with Barton (Figure 3-1) the Schmidt hammer test was used to determine ϕ_r based on ϕ_b as well as estimate the JCS. It was carried out on matrix-saturated joint surfaces, as well as on air-dried smooth sawn surfaces. Matrix saturation was achieved by submerging the samples in water, while air drying was done by leaving the samples on a laboratory table. Each procedure lasted at least twenty-four hours.

Schmidt hammer tests were carried out after the joint surface tilt tests, and when possible on undamaged surfaces of the bottom part of the sample. The procedure included putting the sample in a vice and applying the Schmidt hammer ten times. Results were interpreted by using the average of the five highest values for each set.

In-situ tests were also carried out in the pit. The sample size is naturally larger than in the lab, and the saturation is dependent on weather conditions. Weather during field testing was sunny and dry, but was preceded by rainy days.

Shear box test of joint surfaces

The joint samples were then re-sawn to fit into the available portable shear box device, which limits the sample size to about 100x100 mm. The samples are then set in concrete using the same method as was used for cores by Korpi (2012), holding them with a clamp and protecting the joint edges with low-adhesion tape.

A constant normal loading (CNL) shear box test is carried out by applying a selected normal pressure on the sample. In the case of the used portable shear box device (Figure 3-13 and Figure 3-14) the sample joint surface is positioned horizontally. Thus, the normal load is a combination of gravitational load of the weight of the upper half of the device and sample, and a selected pump-generated load. The normal pressure is determined by the total normal load and the contact area, which is defined as the horizontal cross-sectional area at joint contact.

The test begins by applying a shear load, which induces a shear pressure on the sample. Shear pressure is calculated in the same manner as normal pressure, using the same contact area value. The load is adjusted by the experimenter to keep the shear displacement rate as close as possible to

a selected value, often 0.1 mm / min. This load is recorded at regular intervals to calculate the sample's shear strength, which is the shear stress needed to overcome shearing resistance. Besides the shear displacement, vertical displacement is also measured using dial gauges.

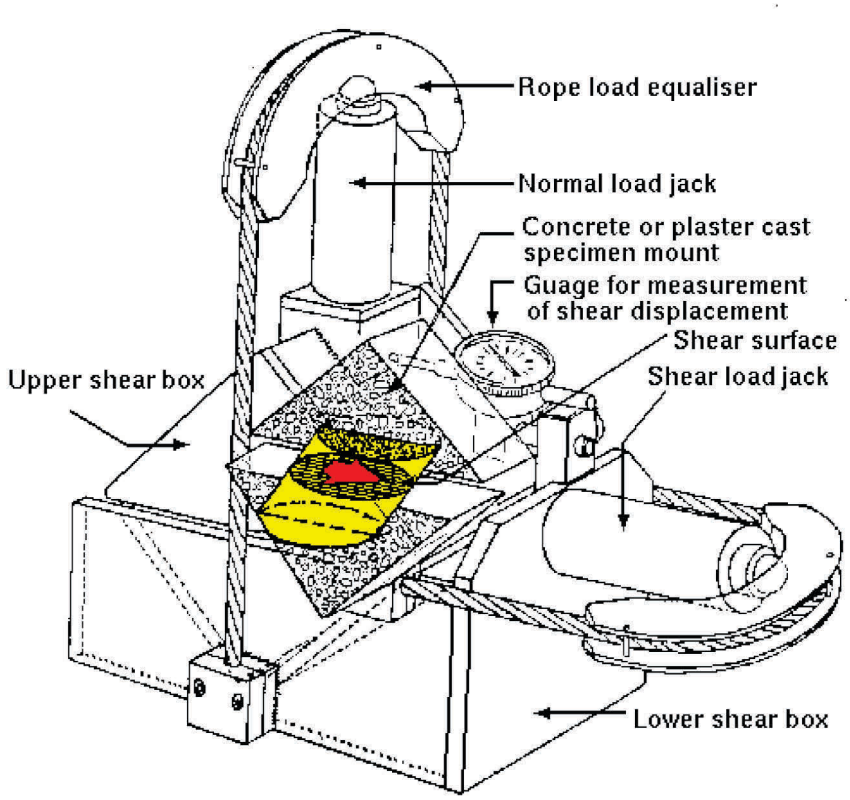

Figure 3-13: Schematic drawing of a portable shear box device (Reeves, n.d.).

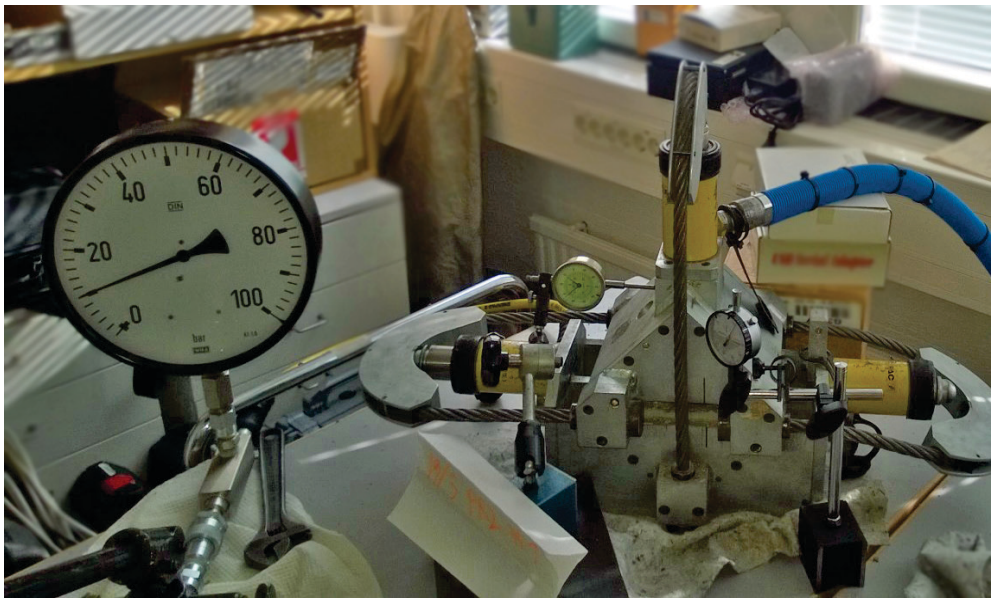

Figure 3-14: Used portable shear box device, shear load pump (left) and displacement dial gauges.

The tests were carried out in accordance with the latest ISRM standard (Muralha, et al., 2013) with the following exceptions due to limitations of available devices:

- Measurements were done using analogue pressure and displacement gauges, thus the pressure readings are accurate to ±5 % at the smallest readings. However, at the peak and residual shear strengths the shear reading is accurate to ±2 % required by the standard.
- The used measurement frequency was once every 0.1 mm of shear displacement (equal to once every minute pre-peak and once every 24 seconds post-peak) due to limitations of analogue devices and human concentration capacity.
- Only one displacement measurement device was used for each displacement direction, and the vertical displacement was measured at the corner and not the centre of the shear box.
- Specimen shape was dependent on available specimens and not all specimens were of a regular shape. Additionally, some samples were too small to provide for a longer bottom part pf the specimen, thus recalculation of the nominal area was required.
- No dummy or pilot tests were carried out due to limited amount of specimens.
- As the normal pressure pump used does not provide fine control over loading and unloading speeds, it was only possible to achieve a loading time of about two minutes, whereas the standard requires it to be five.

The encapsulation material was JB 1000/3 ready-made concrete, which has the strength of 45 MPa after curing 24 hours (Weber, 2015), determined to be large enough to have negligible effect on the test results.

Each specimen is tested up to three times, resetting the sample displacement in between tests. Multiple stage testing (Figure 3-2) was favoured over single-stage testing with multiple samples due to the following reasons.

- The specimens had different sizes and geometries, thus a comparison between the specimens might not be reliable with single-stage testing.
- There was a very limited amount of specimens and it was decided that it is better to get a view of the variation of specimen results than only one single-stage result per specimen. Using single-stage testing would have required a lot more samples and assurance that variability between samples would be low. The obtained results clearly show that sample variability is very high.
- The results produced by a single specimen are more readily comparable with results produced by tests for the BB model on the same samples.

Resetting, as opposed to multiple stage testing without resetting, was selected as the test method. This method includes resetting the specimen to its original location after each test and repeating the test at a larger normal load (Figure 3-2 b). For most specimens, three tests were performed. It has been criticized due to the possibility of asperity shearing and other damage during the first test, which would lower results of later tests. However, normal stresses used in this study are relatively low, and especially the diorite rock has a high strength, so the mentioned risk is small.

The normal pressures were selected to correspond to small-scale slope stability, with the smallest pressure dependent on the minimum pressure provided by the normal pressure pump (0.5 MPa on a d=38mm cylinder) and the weight of the device (20.5 kg) and casted sample (2.7-3.3 kg). Such a small pressure necessitated taking the device and sample weight into account as well. The used normal pressures ranged between 0.09 and 0.58 MPa.

The selected displacement speeds were 0.1 mm/min for pre-peak strength and 0.25 mm/min for post-peak (residual) strength. Example photographs of a specimen before and after testing is provided in Figure 3-15, and an example graphed result set in Figure 3-16.

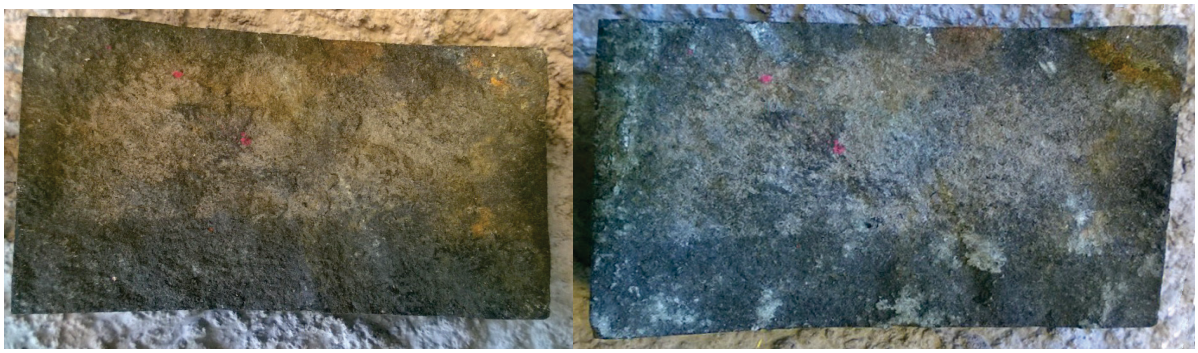

Figure 3-15: Specimen Diorite-2/PR2 (main ramp, diorite), photographed before (left) and after testing.

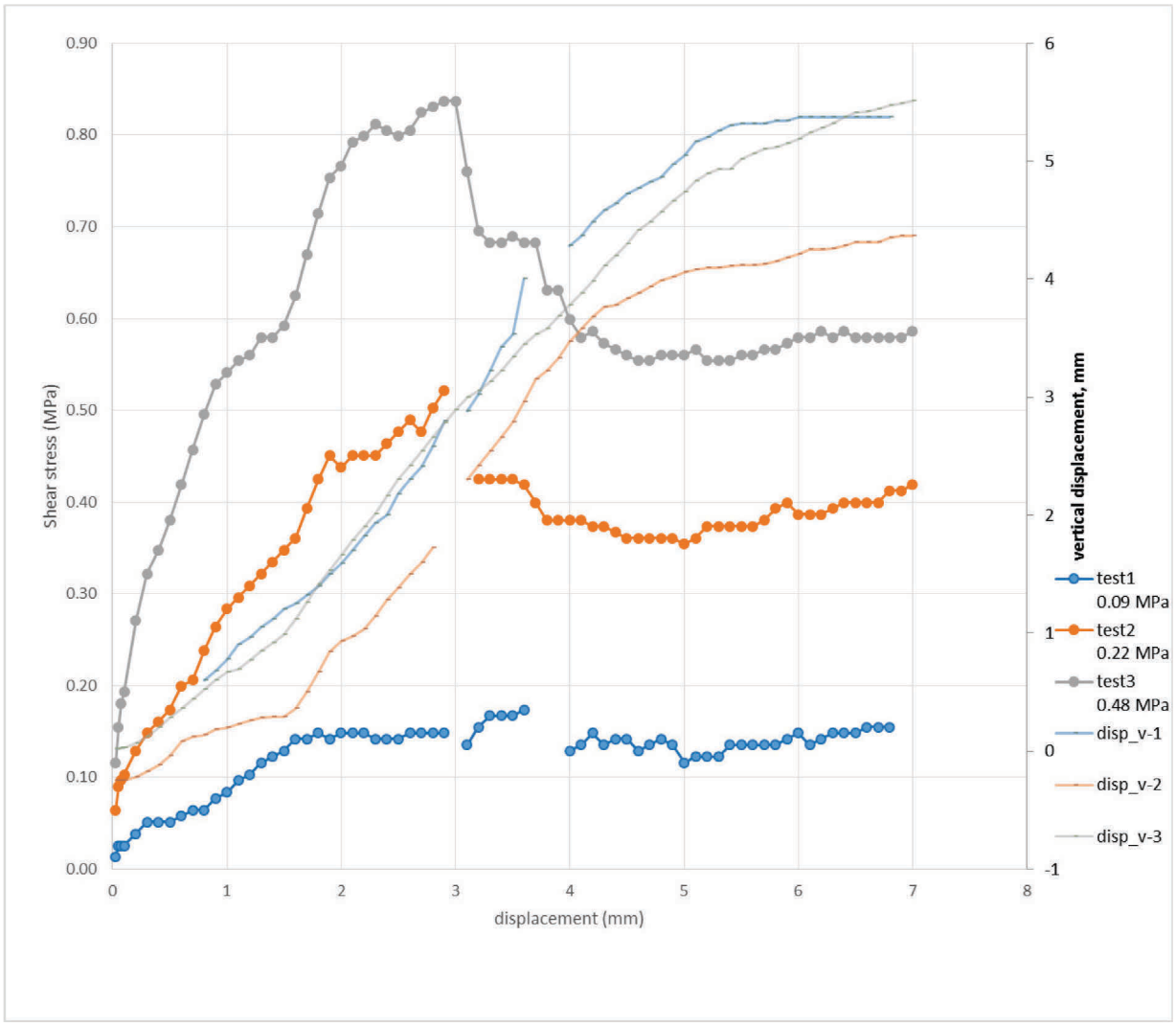

Figure 3-16: A typical result set for a (diorite) sample. The normal stresses for each test are shown on the right-hand side. Some data is missing due to the sample moving several tenths of a millimetre in a short time span.

Sawing of sample for testing

The used samples were of varying size and geometry and needed to be fitted for the testing procedures. Some typical issues are illustrated in Figure 3-17. Sawing was designed to simplify the joint surface geometry for area calculation, and to fit the testing devices. In accordance with the planned testing sequence, the samples were first sawn to fit the tilt table. As the tilt table was large enough to accommodate almost any of the samples outright, sawing was done to create a simple

geometry and a flat base so that the sample would sit evenly on the table. After tilt table and Schmidt hammer tests, the samples were re-sawn to fit the shear-box (100 mm x 120 mm maximum).

When possible, the sample halves were taped together from the side to saw them simultaneously. However, in many cases this was not possible, so the joint surface was somewhat open to water flow from the saw. It is also possible that mechanical vibrations from the sawing process damage the sample surface.

In future research post-extraction sawing should be avoided whenever possible, preferably by using samples that are finalized on extraction, such as large-diameter drill cores which only need to be sawn on the sides and not near the joint surface.

Figure 3-17: Glimmerite sample too large and geometrically complicated to test directly. Besides this, both sides of the sample are partially connected (the sample is at the end of a joint), necessitating sawing regardless of testing capabilities.

3.2 CASE SIMULATIONS

To compare the proposed models, the obtained and selected parameters were used in an initial comparison simulation of an imaginary wedge of slope height (28 m). Swedge rock wedge simulation software (Rocscience Inc., 2015) was used. The lowest laboratory-obtained parameters were selected for initial use, as especially shear box results are expected to overestimate joint strength.

As predicted for relevant stress levels in Figure 4-7, the selected Barton-Bandis parameters produced higher results than the selected Mohr-Coulomb parameters for diorite, and vice versa for glimmerite. More specific results are found in Table 2 and Table 3.

The same parameters were used for further analysis. Discontinuity dip and direction parameters were obtained using 3D photography software 3DM Analyst and 3DM Viewer (ADAM Technology, 2014). Using rock failure reports provided by Yara, failures in diorite and glimmerite were selected for analysis. Later non-failures at visible joint locations obtained from 3D photographs using 3DM software were also analysed. Analysis was done using spreadsheet calculations for plane failures, Swedge for wedge failures and 3DEC (Itasca Consulting Group, Inc., 2013) for a single more complicated failure which occurred during the study.

For known failures exact joint orientations are exposed and thus known. For non-failures simulation and prediction is made difficult by the lack of information on joint continuity. With clearly continuous joints simulation is fairly straight-forward. However, if joints are suspected to be discontinuous the simulation should be built on two theoretical models: one of mechanical behaviour of joints, and another on mechanical behaviour of the massive rock. The effect share of each theoretical model depends on the area of joint continuity out of total possible failure area. It can be assumed that even relatively small areas of non-jointed rock significantly add to the total strength of a proposed wedge failure.

Simulation process

For each simulation, joint orientation was obtained either from failure reports or by measuring the orientation using 3DM software (Figure 3-18). This and slope orientation data was transferred to the relevant software and either model's parameters were input for the calculation.

A safety factor for each input was then obtained through failure simulation and calculation. These factors, and the predictions they suggest, were compared to the failure reports and non-failure status. For failures, the safety factor was expected to be less than or close to 1.0 when dry and less than 1.0 when saturated. For non-failures a safety factor of more than 1.0 when dry was expected. Wet conditions, considered only as an increase in hydraulic pressure, were not compared for non-failures, as it is unclear what the largest hydraulic pressure that has been generated at each joint is.

If these conditions would have failed to be met, the parameters would have needed to be revised in the relevant direction.

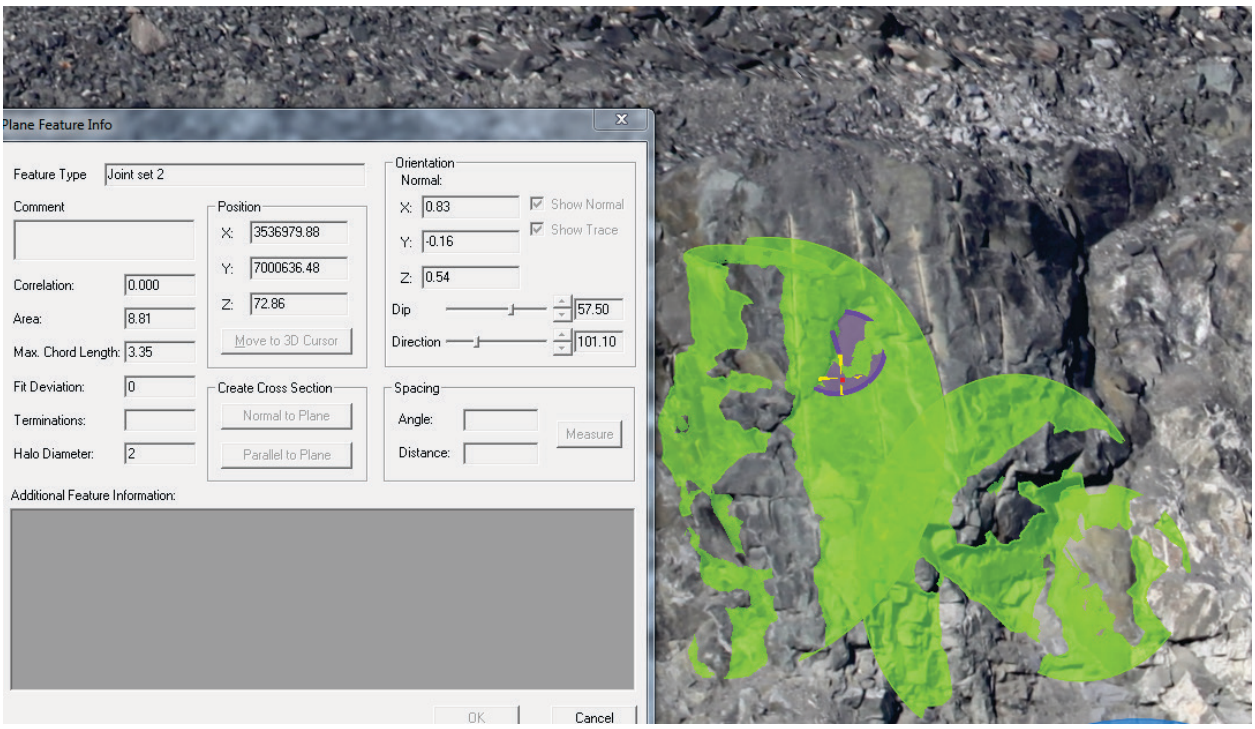

Figure 3-18: Discontinuity directions as viewed in 3DM Viewer. Discontinuity planes, marked using visible discontinuity points, are shown in green. The selected discontinuity plane is shown in purple and its dip and direction are shown in the left-hand box.

Table 2: Simulated sample wedges.

Sample wedges			**Diorite**		**Ore**	
Slope (28 m)	Joint1	Joint2	FS MC	FS BB	FS MC	FS BB
d65 dd 185	d45 dd125	d70 dd225	1.26	1.51	0.76	0.74
d65 dd 185	d37 dd157	d32 dd226	1.68	1.90	1.01	0.93

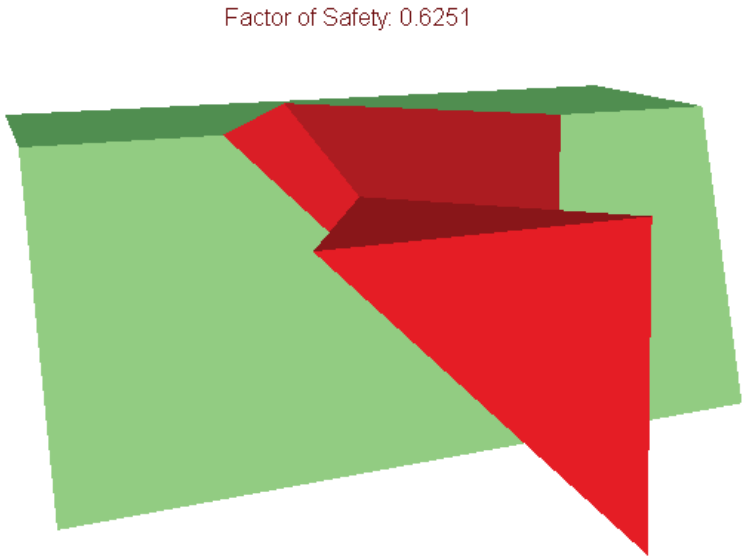

Figure 3-19: Sample wedge simulated in Swedge software.

Table 3: Simulation results of failures and suspected failure areas.

Software	Name	Date	Type	Rock	Size ~ m3	FS MC	FS BB	Disturbances	FS expected	FS expected with disturbances	notes
spreadsheet	SW 66-52	31.7.2014	Wedge	diorite	2	0.69	0.99	no	**0.99**	<<1	
Swedge						0.69	0.97				
n/a	W-74-46	20.7.2014	block	?	10	n/a	n/a	blast	0.99	**<<1**	
Swedge	NWR road	27.3.2014	block	ore	9	0.92	0.97	no	**0.99**	<<1	Difficult to model
n/a	NW 52	27.10.2014	?	?	10	n/a	n/a	rain	n/a	**<1**	
spreadsheet	ST	11.10.2014	plane	ore	8	0.27	0.28	rain	1.1	**<<1**	Likely cohesion due to discontinuous joints
Swedge	NW 52	7.4.2014	block	ore	5	0.1	0.11	no	**0.5**	<<1	
spreadsheet	SW 10-24	29.9.2014	plane	ore	5	0.14	0.14	no	**0.95**	<<1	
3DEC	Main ramp	4.6.2015	blocks	ore	?00	0.8-1.0			**<1**	<<1	
spreadsheet	NW1-big	nan	taso	diorite	>100	1.45	1.64	no	>>1	>1	
Swedge	SW 66-52	nan	wedge	diorite	~20	0.69	0.93	?	~1	<1	joint continuity?

4 RESULTS AND COMPARISONS

This section presents the laboratory-obtained parameters for both the Mohr-Coulomb model and the Barton-Bandis model. These are compared, and unexpected findings on the joint roughness coefficient JRC are presented. The parameters selected as the starting point of back-calculation are presented and motivated, and a brief conclusion on their validity is stated. The presented results are discussed, while more extensive methodology discussion is left for section 5.

4.1 MOHR-COULOMB MODEL PARAMETERS

The results obtained by different methods vary largely and are shown below. The shear box results are directly related to sample properties at different normal stresses and can be assumed to follow a curvilinear, possibly log-linear (Barton, 1981), shear failure envelope (Figure 4-1), such as the Hoek-Brown (Hoek, et al., 1992) and Barton-Bandis models. The tangent fitting of these models creates a high ϕ and low c at low normal stresses, and vice versa at high stresses. The linear fitting of test results produces parameters applicable for the stress levels the tests were done at.

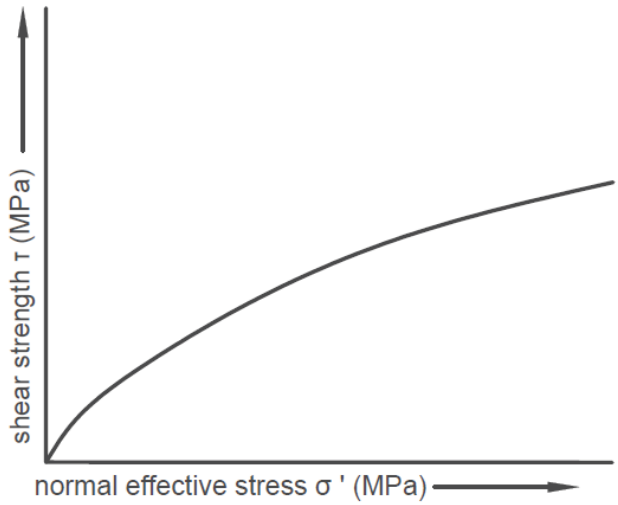

Figure 4-1: Sample Hoek-Brown curve for jointed rock masses (after Hoek, et al., 1992, p. 8).

Literature values

Literature values for MC joint parameters are rare, as the MC model was not developed specifically for joints. However, some comparable values are found in the Open Pit Slope Design book. Fine-grained igneous rocks, which the Siilinjärvi diorite represents, have a residual frictional angle of 33-52 degrees with zero cohesion (Franklin & Dussealt, 1989; via Karzulovic & Read, 2011, p. 100). This is in line with the shear box results (ϕ_{res} = 40.2-64.3 degrees), as the sample scale effect described in section 1.2 would create higher strength values for shear box samples than in-situ blocks. The closest literature value to chlorite-filled glimmerite is noted as “foliation plane with chlorite coating in a chloritic schist”, which may or may not be representative. The parameters are marked as c = 0 and ϕ_{peak} = 33-36 degrees, which is somewhat comparable with shear box results (ϕ_{peak} = 29.8-42.2 degrees, excluding the least representative sample).

MC fitting of shear box results

The most direct method for obtaining Mohr-Coulomb parameters used in this study is linear fitting of shear box test results. MC fitting results obtained via other methods, described below, are compared to these.

Linear fitting was based on shear box and joint tilt test results for each sample. Despite generating more data by adding the initial joint tilt tests as data points, such combining may be criticized due to data from two different test types being interpreted in the same way. Though such critique may be theoretically correct, it is meaningless in view of this study for two reasons. First, the difference between linear fits with and without the joint tilt test data is low: 2-69 kPa for cohesion and 0.21-3.18 degrees for friction, with larger absolute values corresponding to rougher samples. Second, the gained values are not used directly. Instead, they are used as input for back-calculating usable parameters from known failures and non-failures.

The shear box results are presented below in Table 4 and Figure 4-2, Figure 4-3 and Figure 4-4. The sample strength varied by a factor of two to three for both diorite and glimmerite samples. In both rocks the sample with the lowest measured roughness (JRC) also produced the lowest shear strength results in shear box testing. Higher sample JRC also correlated with higher results, with one exception in diorite. The sample with the highest JRC (labelled LLW or Diorite-3) produced a lower result than would be expected based on the JRC and two first tests. Possible reasons for the variability are discussed in section 5: Discussion and suggestions, as is sample representativeness.

This decreased result could be explained by the sample JRC measurement being highly affected by a large asperity at the front of the sample, which broke off towards the end of the second test of the three-test series, likely causing a large decrease in shear strength. This is somewhat unavoidable in multi-stage shear box testing of samples with large singular asperities. However, explanations made in hindsight need to be approached with caution, and more data would be needed to confirm this hypothesis.

Table 4: Variation of fitted shear box results, in the form of $\tau = \boldsymbol{c} + \sigma_n \tan\boldsymbol{\varphi}$. Note that cohesion is given in kPa instead of MPa.

	$\tau_{peak\ min}$	$\tau_{peak\ max}$	$\tau_{res\ min}$	$\tau_{res\ max}$
Diorite	-0.1 kPa + σ_n tan41.7°	25.3 kPa + σ_n tan65.6°	-11.3 kPa + σ_n tan41.1°	-34.5 kPa + σ_n tan63.4°
Glimmerite	0.1 kPa + σ_n tan29.8°	57.3 kPa + σ_n tan55.1°	0.1 kPa + σ_n tan28.2°	48.1 kPa + σ_n tan50.6°
Shear zone	3.8 kPa + σ_n tan26.5°		-0.9 kPa + σ_n tan25.9°	

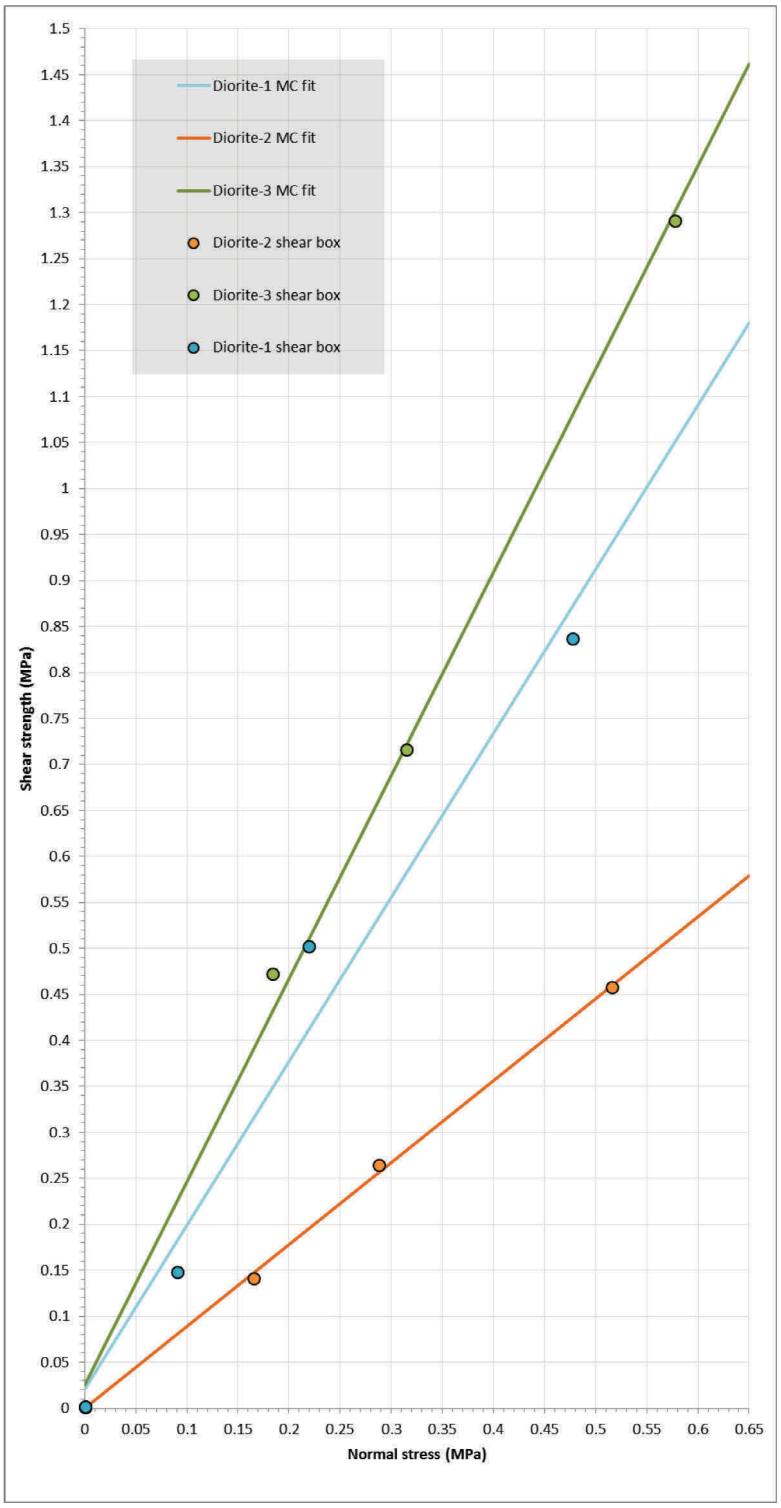

Figure 4-2: MC fitting for peak strength of three diorite shear box test sets, with three tests for each sample. Each colour represents a single sample, with each line representing an MC fit and each point a shear box test result.

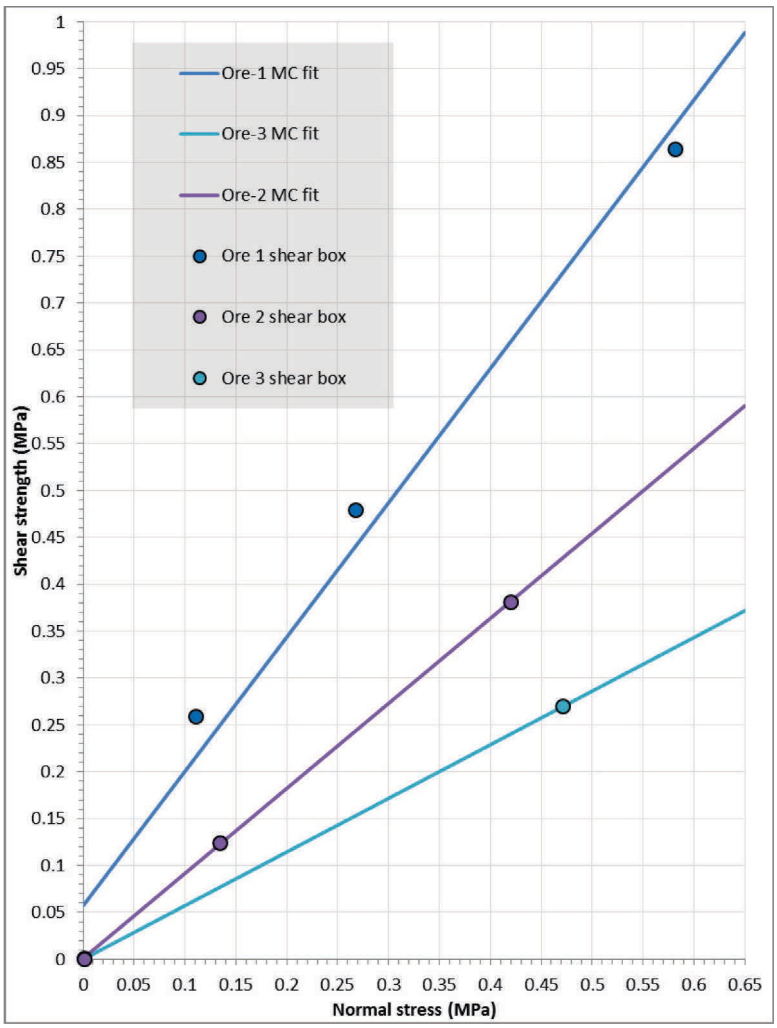

Figure 4-3: MC fitting for peak strength of three glimmerite shear box test sets. Each colour represents a single sample, with each line representing an MC fit and each point a shear box test result.

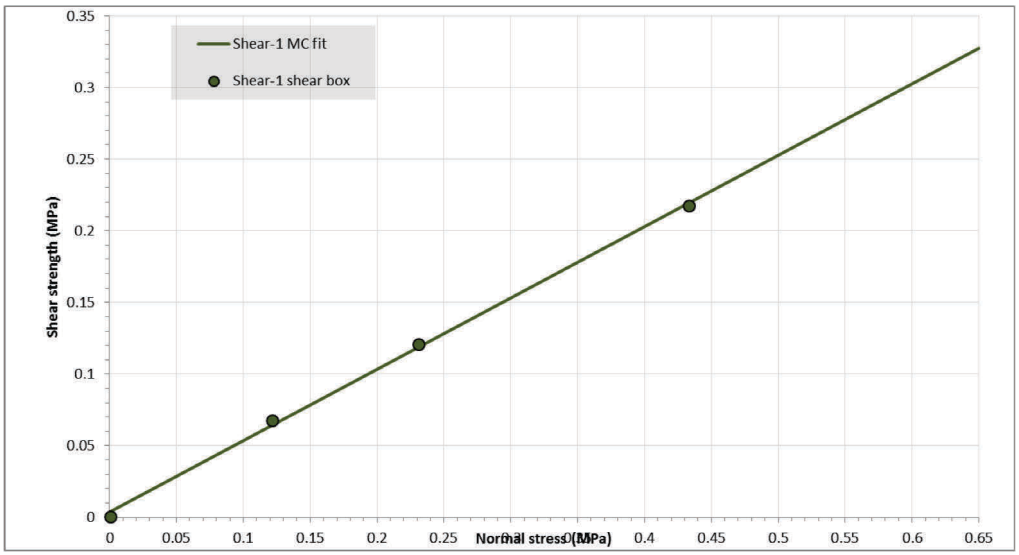

Figure 4-4: MC fitting of peak strength for shear zone sample shear box test set.

4.2 BARTON-BANDIS MODEL PARAMETERS

Each of the three Barton-Bandis model parameters was obtained for the samples using laboratory and in-situ tests. While estimating the joint compressive strength and residual friction is fairly straightforward, indirect tests for determining the joint roughness coefficient yielded data that was not simple to interpret. The most relevant values were selected for back-calculation and are summarized in section 4.5.

Joint roughness coefficient JRC

JRC values obtained using roughness profiles and laboratory testing shown in the tables below.

Table 5: JRC comparison for diorite. Sample amounts: lab sample n=6, in-situ n=3, tilt n=6.

	Low		High		Mean	
Method	Lab	In-situ	Lab	In-situ	Lab	In-situ
Subjective profiling	6.3	1.7	12.0	5.7	8.6	3.4
Asperity height profiling	7.2	6.8	20.0	10.5	14.3	7.3
Joint tilt test	5.0		6.1		5.6	

Table 6: JRC comparison for glimmerite. Sample amounts: lab sample n=6, in-situ n=3, tilt n=6.

	Low		High		Mean	
Method	Lab	In-situ	Lab	In-situ	Lab	In-situ
Subjective profiling	3.5	1.0	15.3	3.0	8.2	1.8
Asperity height profiling	7.0	4.5	20.0	8.6	13.3	5.9
Joint tilt test	4.2		11.5		6.4	

The subjective method produced clearly lower results, and the laboratory test results are even lower. In-situ JRC values are lower than those of samples. These phenomena are discussed in 5.2: JRC comparisons.

Joint compressive strength JCS

The preliminary JCS (r) value, based on Schmidt hammer tests, is between 74 % and 100 % for diorites and between 83 % and 90 % of the UCS (R) Schmidt hammer rebound values. With used UCS values being 217 MPa for diorite and 28 MPa for ore (Table 1), JCS is assumed to be 160-217 MPa and 23-25 MPa respectively. Hard chlorite filling in glimmerite may however raise the JCS value.

Residual friction ϕ_r

The diorite core samples obtained close to the two sample locations gave a basic friction angle of 29 degrees (main ramp west) and 31 degrees (southwest) degrees. This is in line with literature values of 31-35 degrees for granites (Barton, 1973; Barton & Choubey, 1977; via Karzulovic & Read, 2011, p. 106). ϕ_r was calculated to be between 24 and 31 degrees, determined by Schmidt hammer rebound value difference between flat rock and joint surfaces. As the joint surfaces are essentially unweathered, it is likely that the lower ratio is due to specimen size and holding (i.e. testing errors).

With glimmerite determining residual friction is somewhat trickier. The basic friction angle for glimmerite was determined to be 18.7 degrees, while determining the basic friction angle of the thin

chlorite surface is not possible with conventional tilt tests. Determining the combined effect the basic friction angles for glimmerite and chlorite is even more challenging, as it would be dependent on chlorite coating thickness and susceptibility to shearing during failure. The friction angle for glimmerite is used as a starting point and the same methodology for determining ϕ_r is applied for both rock types. Thus ϕ_r for glimmerite is between 15.3 and 16.8 degrees.

4.3 OBTAINING MC PARAMETERS VIA BB RESULTS

Instantaneous c and ϕ for any normal stress can be obtained using BB results by fitting a tangent line to the BB curve at that normal stress. This is only necessary if the simulation software being used does not already include the BB model. As this study deals with a low range of normal stresses and relatively low JRC values, which creates a curve which is already nearly straight, it is easier to compare BB and MC results directly, which is carried out below in section 4.4.

4.4 COMPARISON OF MC AND BB RESULTS

Results of MC and BB models were compared within the range of used normal stresses (0-0.65 MPa). The comparisons are presented in Figure 4-5 and Figure 4-6. The figures contain a fitted MC line for each sample, based on shear box and tilt tests. Dashed lines represent BB curves for each sample, and single points represent shear box or tilt test results. Curves and points of the same colour represent the same sample.

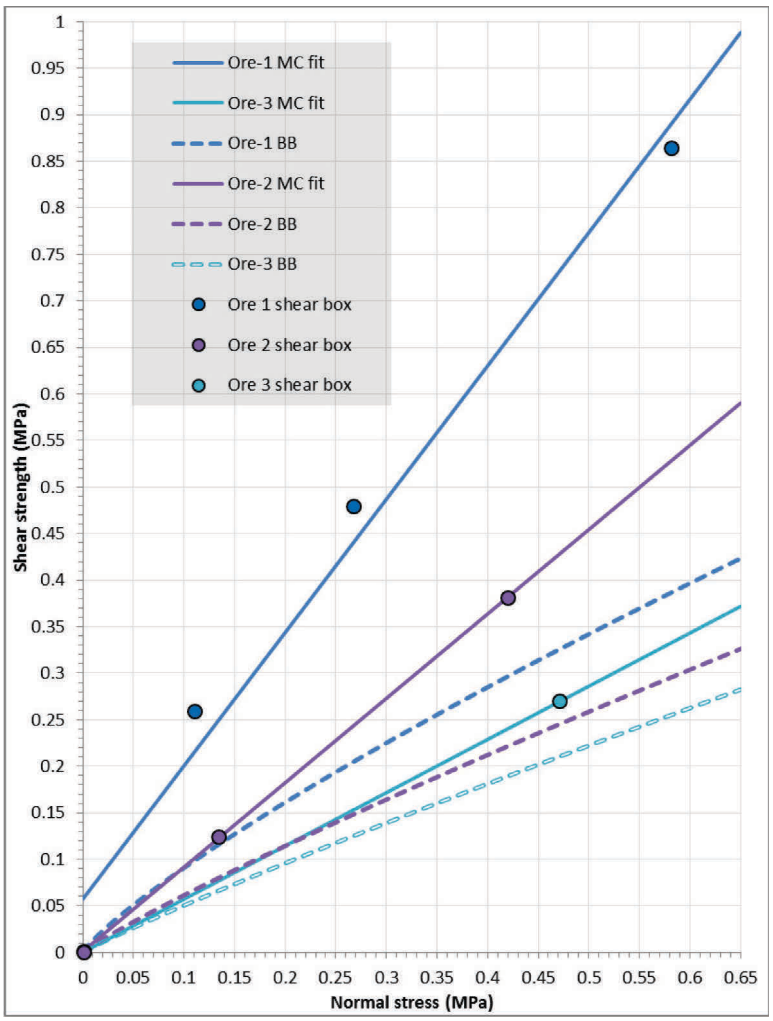

Figure 4-5: MC-BB comparison for glimmerite ore samples with shear box results. Each colour represents a single sample, with each line representing an MC fit, each dashed line the BB curve and each point a shear box test result.

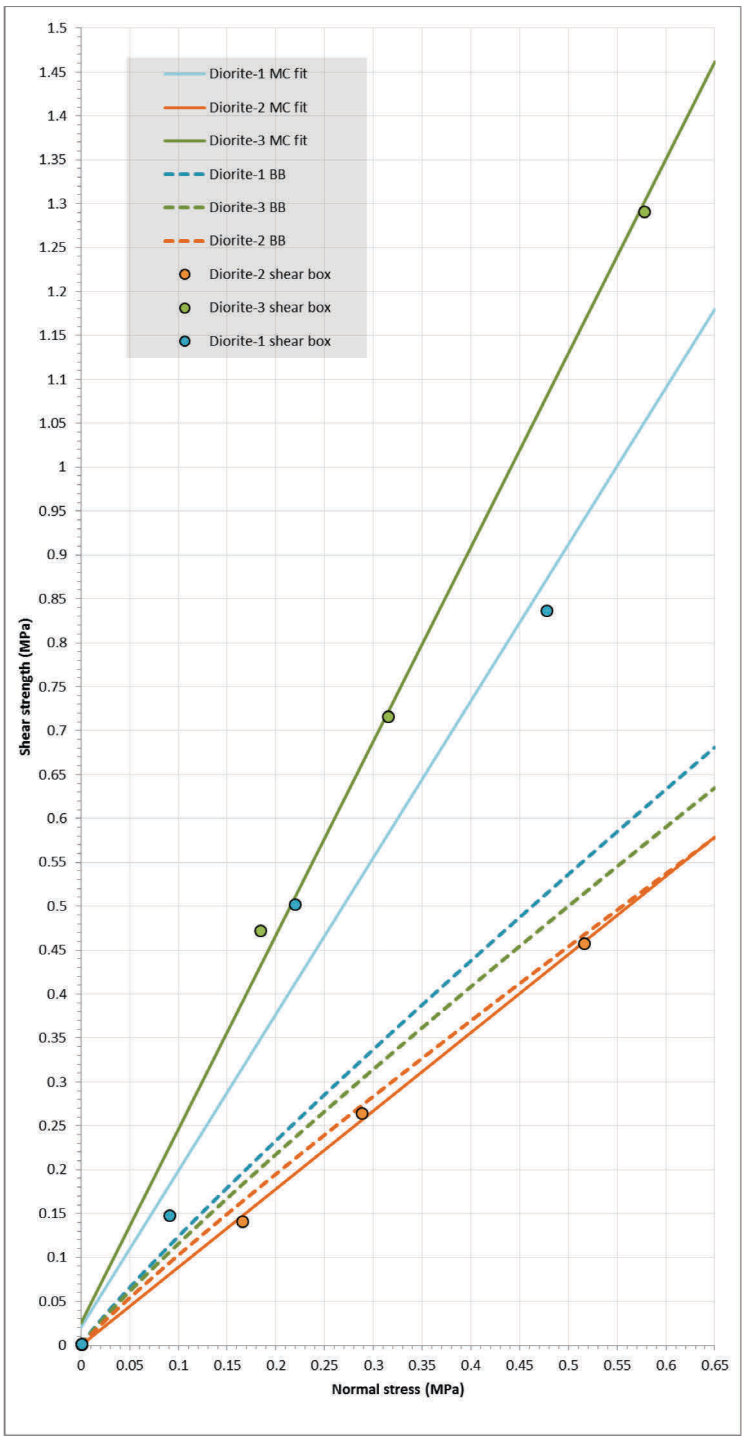

Figure 4-6: MC-BB comparison for diorite ore samples with shear box results. Each colour represents a single sample, with each line representing an MC fit, each dashed line the BB curve and each point a shear box test result.

Another comparison was done between MC and BB results for the weakest samples of each rock type, and a range of BB results using in-situ profiled JRC_0 variability and laboratory ϕ_r result variability (Figure 4-7). While MC and BB results for the weakest diorite sample fall within the variability range, even the weakest ore sample produces a result above the given variability range. This suggests that all the used glimmerite samples were rougher than the relevant in-situ joints. One influencing factor is sample size, as this was a small core sample, so even higher shear box results than from block samples could be expected. Another factor is sample JRC_0, which was estimated to be 3.5, whereas the high end of in-situ measurements in the relevant direction is $JRC_0 = 1.33$.

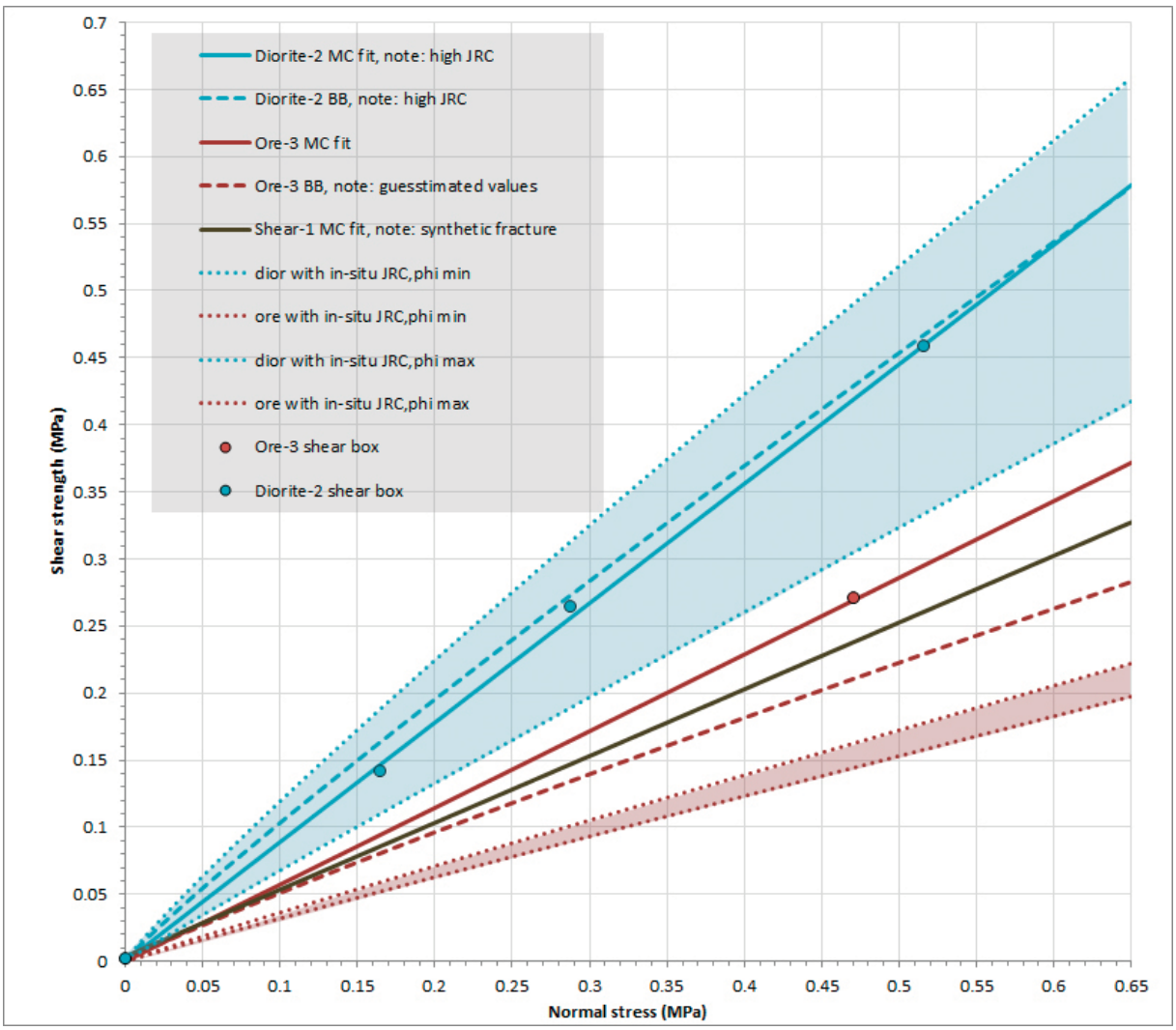

Figure 4-7: Visual comparison between lowest MC (solid line) and BB (dashed line) results for ore (red), diorite (blue) and shear zone (green), as well as the spread of ore and diorite BB results when using the φ_r spread of laboratory results and JRC_0 spread of in-situ profiling measurements. Possible joint matching issues are not considered in the spread, meaning that the lower end of the spread may be overestimated.

4.5 SELECTED PARAMETERS FOR SIMULATION

Considering that at small sample sizes used in testing the effect of asperities is higher than for in-situ block sizes, the lower end of the Mohr-Coulomb shear box results, with less asperity effect, is likely to be better suited for use in simulations. This assumption is also supported by results of BB fitting.

Variability of Barton-Bandis model results (Figure 4-5 and Figure 4-6) is relatively low, while issues with sample representativeness are of high importance. Thus BB parameters were selected based on the representativeness of samples they were obtained from. Representativeness in turn was estimated based on visual comparison to in-situ joints. JRC values obtained by profiling methods were ignored and instead values obtained from tilt tests were used.

The initial selected parameters are shown below (

Table 7).

Table 7: Parameters selected for simulations.

	Mohr-Coulomb		Barton-Bandis		
	c (MPa)	ϕ (deg)	ϕ_r (deg)	JCS (MPa)	JRC
Diorite	-0.0001	41.7	28.5	200	5.3
Glimmerite	0.0001	28.2	16.8	25.3	4.2

Validity of selected parameters based on known failures and suspect structures

Based on simulation results of several failures and suspect areas which have not failed (Table 3), the preliminary verdict is that the selected parameters are valid for simulations. Overall the amount of data is limited and more failures and suspect areas need to be found and simulated.

It seems that joint continuity has more effect on the failure results than parameter variability, especially in the case of small ore blocks. Thus, any method of evaluating the continuity of joints at a suspect area is crucial to the resulting strength and failure probability estimates.

5 DISCUSSION AND SUGGESTIONS

The conducted research has produced preliminary results for comparison of the Barton-Bandis and Mohr-Coulomb models in small-scale joint stability simulation. Various research issues were identified, including sampling methodology, amount of gathered data in relation to parameter variability, and model adequacy. These and suggestions for future research and simulation methodology are discussed below.

The joint roughness parameter proved to be more complex than what Barton's suggested research methods implied. Related findings and suggestions are also discussed in this section. Finally, the preliminary model results are compared and the related model usefulness is analysed.

5.1 DRAWBACKS OF SAMPLING, TESTING AND ESTIMATION METHODS

Any laboratory-scale test is bound to both limited sample sizes and at least somewhat disturbed samples. Besides this, both used models are of course merely proxies for a complex reality (MC being a largely simplified theory, and BB being partly empirical in nature). Some drawbacks of the methods used in this study are noted below. These include biased sample selection, imperfect sample handling, sample size relative to in-situ block size and issues with joint roughness estimation.

Sample properties and selection bias

In general, the size and shape of the joint samples was varied. This variability alone makes results somewhat more difficult to interpret and scale. It is also difficult to determine the nature of the possible joint filling, as sample selection was not unbiased and the samples were not always perfectly protected for transportation.

The small sample size is not representative of the considerably more continuous in-situ joints. Usually small sample size produces artificially high values of shear strength compared to in-situ behaviour. Additionally, laboratory-scale samples ($L < 200$ mm) produce significant result variability in both physical and numerical shear box tests due to local variability in effective roughness (Bahaaddini, et al., 2014, p. 220). This variability effect is also seen in this thesis study. Notably for large joints the *peak* strength may be lower than even *residual* strength measured from small samples. On the other hand, unusually planar (low JRC) joints may be essentially unaffected by the scale effect from sample size. (Barton, 1981, pp. 171-177).

In any case small samples only represent small-scale roughness and don't account for undulation and other larger-scale roughness, which may be higher or lower than small-scale roughness. This could be further investigated by adapting the a/L profiling method to larger scales.

Another limitation of testing single samples is that the response of the surrounding rock mass, which affects joint matching after beginning of shearing, is absent. The effect on joint matching depends on whether the individual blocks are able to lock into their shear paths or if they are pushed off that path (to lower matching) by the surrounding rock mass (Barton, 1981, p. 180). However, this has little effect on studies of wedge failures.

An on-site visit in April 2015 revealed that the provided samples were highly unrepresentative of the relevant joint surfaces. JRC_0 values varied between profiling of laboratory samples and in-situ profiling. These roughness values for diorite samples were between 8 and 12, whereas in-situ measurements on the west side provided values of 1.5 to 5.5 depending on direction. For glimmerite the corresponding values were 3.5 to 13.5 for samples and 1 to 3 in-situ. All the used samples were collected from post-blast or post-collapse areas. In such areas, joint samples that have survived the

mechanical stress are unlikely to be the weakest links of the rock mass. This suggests that a disadvantageous selection bias was at work in sample gathering.

More samples were collected during the visit with a focus on attempting to find more representative samples using visual evaluation. Of course this alone does not completely remove the selection bias.

Another attempted method to avoid selection bias was to use drill core samples. The main issue with using these samples is the relatively small size of the joint surface area. A small contact area makes results more variable and difficult to interpret. It was attempted to maximize the usable joint surface area by selecting cores which cut through the joint diagonally. This backfired as the diagonal joint samples sustained damage and discing (Figure 5-1) during the casting process, leaving only one somewhat usable core sample to test.

Another issue with the small contact area provided by core samples arises due to physical limitations of the shear box device. The smallest normal load reliably produced by the shear box device is 570 N. With joint contact areas of 1000 to 2000 mm^2 this corresponds to σ_{no} = 0.3-0.6 MPa. This makes it impossible to carry out tests corresponding to failures at the smallest scale of interest, which would start at less than 0.1 MPa.

Figure 5-1: Sample discing, as well as fracturing due to part of the core sample hanging in the air above the concrete casting.

Sample degradation

The used samples had to be worked on in multiple stages prior to testing, exposing the joint surfaces to degradation risk. Degradation occurs when joint filling and any soft or brittle rock is removed by external forces. The samples were exposed to mechanical stress during and before collection, as some were collected from post-collapse sites and others were removed from the surrounding rock mass using a sledgehammer as carefully as possible. For transportation the samples were padded to avoid damage. However, not all joints were taped to protect the filling.

In the laboratory, degradation risks involve dynamic mechanical stress from sawing and wet-dry cycles due to submersion in water to achieve matrix saturation. Due to the limited amount of samples, each sample was sawn twice - first for the joint tilt test, preserving the maximum possible joint contact area, then re-sawn to fit the shear box device.

Barton-Bandis JRC estimations

JRC_0 estimation is subjective, as it requires visual comparison between a very scarce range of standard profiles and the profiles attained using a profilometer. Additionally, the profilometer accuracy (size of comb teeth) affects the perceived small-scale roughness. The JRC a/L method, on the other hand, while being objective, only takes the largest-scale roughness into account. It completely ignores any smaller scale roughness and undulation. This means that it is likely only suitable for use after being adjusted separately for different rock types.

According to the original report (Barton, 1981), the log-log scale sheet (Figure 3-6), used for the a/L method, is based on earlier roughness profiles of 10 cm long joint samples and tests on model replicas of different roughness. The roughness profiles used to develop the method are based on aplite, granite, hornfels, calcareous shale, slate, gneiss and soapstone samples (Barton & Choubey, 1977), none of which properly represent the rock types studied for this thesis. It is not made clear how much these samples deviated from the results of the proposed method, or if the deviation was different for different rock types.

Either of the profile estimation methods is unable to take joint matching into account, as only one side is profiled at a time. This likely produces higher JRC results than tilt testing, which inherently includes JMC in the calculated JRC result. Tilt testing is recommended as the more reliable method (Barton, 1981).

For in-situ measurements any possible joint surface degradation due to exposure to weather could not be taken into account, however based on visual assessment the damage was minimal. More importantly, however, joint matching cannot be measured on exposed joints and any loose joint filling has likely been lost quickly during and/or after exposure of the surface.

Barton-Bandis core tilt tests

Tilt tests of cores, used to determine ϕ_b, can only produce the upper bound of ϕ_b, as any roughness/undulation dependent on the core drilling device will create a larger result.

Barton-Bandis Schmidt hammer tests

Schmidt hammer results at laboratory scale are at least somewhat dependent on sample size as well as how the sample is held in place. It is recommended to do in-situ measurements, which are both simpler and likely more reliable due to practically unlimited sample sizes.

However, in-situ measurements suffer from decreased amounts of joint filling, which may or may not have existed. Waiting for matrix saturation conditions can also be difficult and unpredictable. The effect of block size can generate the necessity of doing R-tests (dry, sawn surfaces) on large blocks as well, which would need to be obtained separately.

The actual difference, let alone relationship, between in-situ and laboratory measurements is not clear with the limited amount of data (Figure 5-2 and Figure 5-3) and needs further investigation.

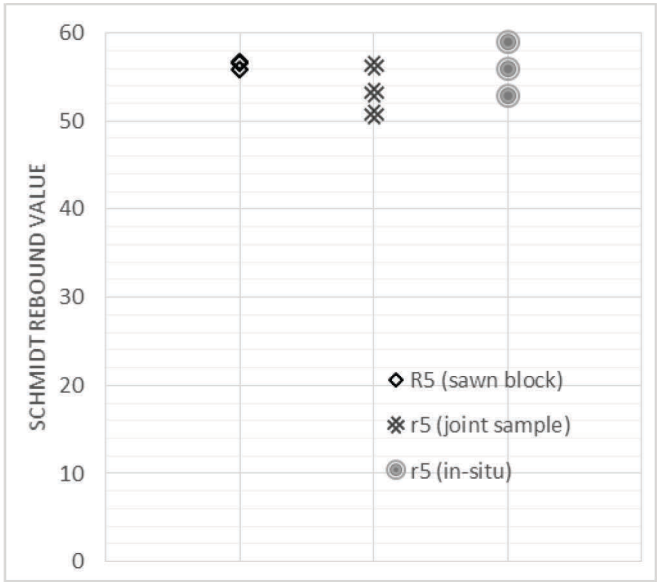

Figure 5-2: Diorite Schmidt hammer test results.

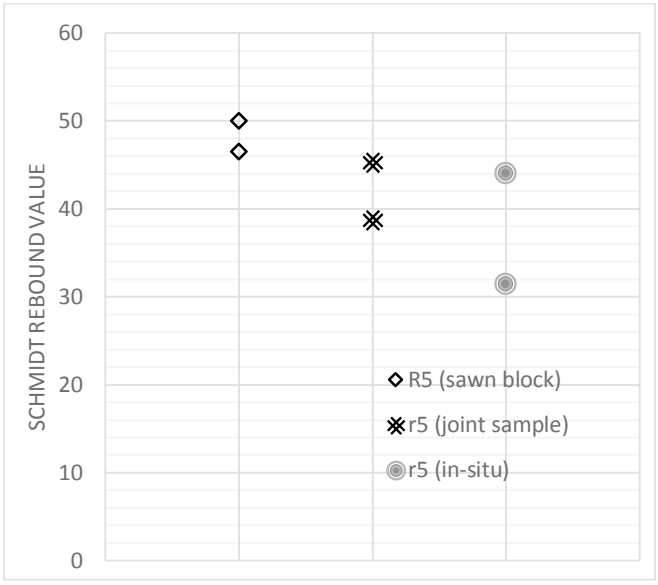

Figure 5-3: Glimmerite Schmidt hammer test results.

ϕ_r values derived using the results may not be exact. However, this is compensated somewhat by JRC results. as the obtained/selected residual friction angle affects the JRC result obtained from tilt tests.

The Schmidt hammer used in the study had to be serviced in the course of the study. Calibration tests using large saw-cut rock blocks before and after servicing did not show any significant difference, thus results from different time frames are assumed to be equally reliable.

Mohr-Coulomb shear box tests

Besides the drawbacks mentioned in sample properties, the shear box method in itself has its limitations. For one, the limited sample size creates a larger effect of the asperity and geometrical components of shear strength than could be expected for the full-length discontinuity (Bandis, et al., 1981). The variability of these components also creates variability in the actual test results, creating a need for more data points.

Multi-stage testing creates damage to the surface, which can cause somewhat lower shear strength results with each progressive test than there would be in a single-stage test.

Mohr-Coulomb fitting of shear box tests

Fitting the shear box test results on linear scale leaves some spread between predicted shear strength and the original results. However, for all datasets $R^2 > 0.95$ and the average absolute deviation of shear strength is between 0 and 0.045 MPa, which are deemed insignificant for design purposes.

A natural drawback of shear box testing (besides sample size) is that the results are only applicable within the used stress range (thus the used stress range was selected to apply to slopes of h < 30 m).

A possible correlation can be observed between JRC (especially JRC_0 determined by profiling) and data spread (Figure 5-4), which could be explained by larger asperities, which create a random-seeming effect on results due to naturally uneven spread of the asperities themselves.

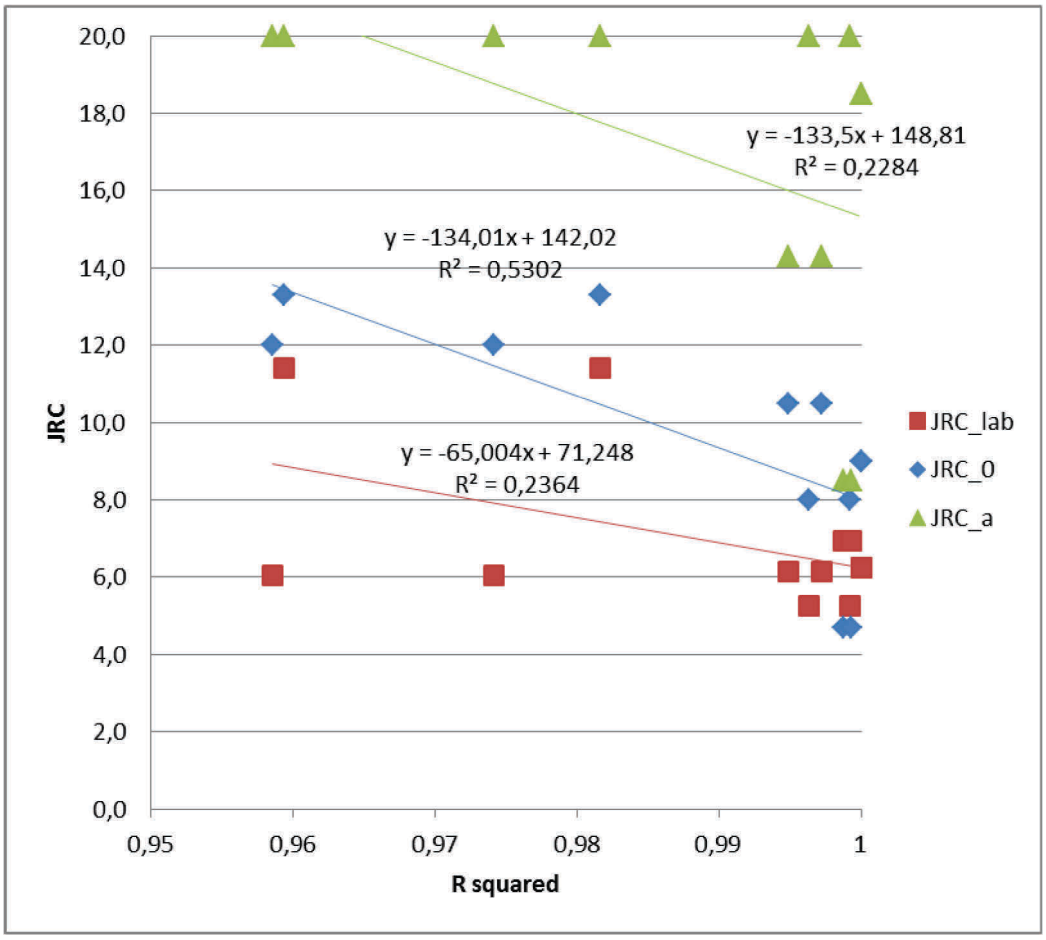

Figure 5-4: Relationship between JRC and R^2. The R^2 (correlation of correlation) values shown here are for correlation between JRC and R^2 (correlation of SB data)

5.2 JRC COMPARISONS AND OBSERVATIONS

Different methods of obtaining the JRC parameter of the BB model yielded significantly different results. The joint tilt test results rendered the smallest JRC values. When profiling, a/L JRC results of the same profile rendered significantly larger JRC values than the profile comparison method. These larger results were deemed to be unrealistic due to being far off the joint tilt test results.

The profile comparison and a/L methods were thought yield similar results. However, this study demonstrated that the a/L method can be expected to yield different results for different rock types

and may need to be scaled by rock or joint type. This is due to a fundamental difference of the methods: profile comparison, albeit subjective, is based on the full shape of the profile. The a/L method, on the other hand, is based on the vertical distance between the single highest asperity and single lowest dimple of the profile. Thus profiles with contrasting roughness characteristics may yield the same result (see Figure 5-5).

Table 8: Comparison of methods of obtaining the JRC parameter through profiling.

Profile comparison	Subjective, often repeatable; based on a comparison made by a human mind	Makes an estimation based on the visual appearance of the whole profile
a/L measurements	Objective and repeatable: based on measurements	Makes an estimation based on two extreme data points of the profile

Figure 5-5: Two joint profiles which would yield the same result using the a/L method, yet are likely to have very distinct mechanical characteristics. Above is Barton's comparison profile for JRC=8-10, below a version edited for illustration purposes.

The original hypothesis for the a/L method is that in any rock type, mechanical joint roughness characteristics correlate directly to the maximum asperity height difference (parameter a). This hypothesis is shown to be wrong both by the simple example above (Figure 5-5) and comparison data in this study, shown below in Figure 5-6, which includes a preliminary linear fitting of the existing (albeit limited) data to convert from $JRC_{0,a/L}$ to the more realistic $JRC_{0,profile}$.

Here, an updated hypothesis is proposed that *in **a given area** and for **a given rock** type roughness characteristics are proportional to the maximum asperity height*. The a/L method log-log sheet (Figure 3-6) provided follows equation 5.2-1. Correlation of asperity height and JRC specific to each rock type should be investigated to correct parameters for the equation.

$$JRC = \frac{a}{2.2 \cdot L^{0.95}} \qquad 5.2\text{-}1$$

Approximate equation used for the JRC a/L method, with constant parameters in the denominator (factor and exponent of the length L).

Note that asperity height a is in millimeters and length L Is in meters.

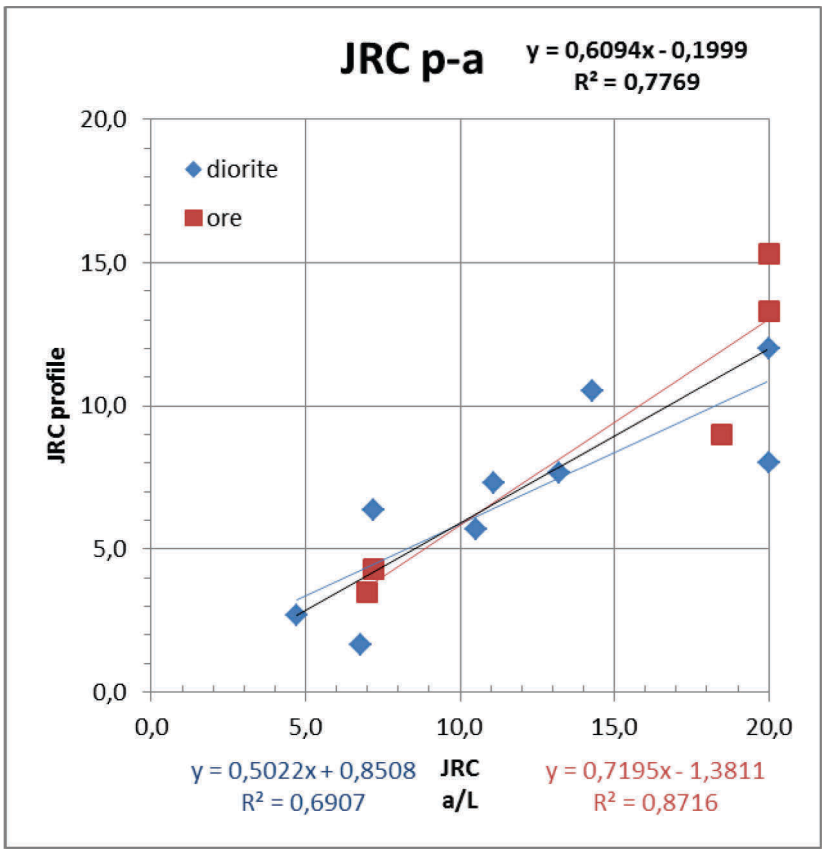

Figure 5-6: Linear fitting of relationship between $JRC_{0,a/L}$ and $JRC_{0,profile}$ for or, diorite and both. The suggested relationship needs further research to be validated. JRC p-a stands for comparison of JRC data obtained from profile comparison (p) and asperity height (a) methods.

Profile and laboratory JRC comparison, matching considerations

JRC values obtained using profiling and calculated values based on tilt testing also did not match, with profiling consistently producing a higher value than lab testing. One possible explanation, besides the subjectivity of the profiler, is that the joints are not perfectly matching.

Joint matching in relation to roughness and the JRC parameter has been introduced by Zhao (1997a) as the joint matching coefficient (JMC), which represents the portion of joint surface area where opposite sides are in contact (Figure 5-7).

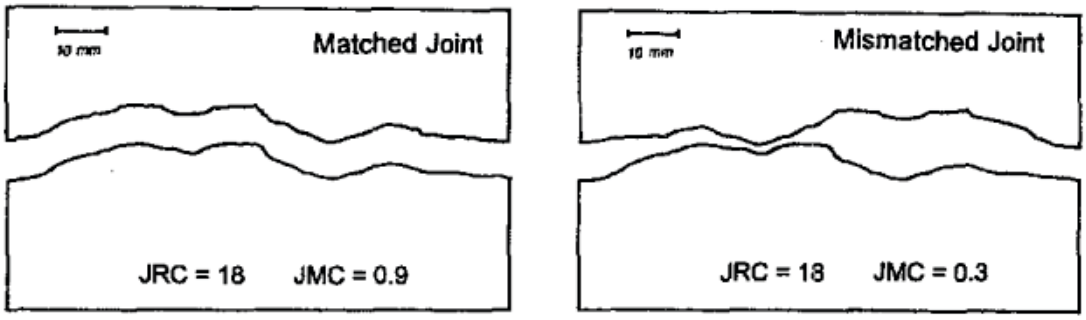

Figure 5-7: Concept of joint matching (Zhao, 1997a).

It is proposed (Zhao, 1997b) that the JMC parameter should be taken into account as a direct coefficient of JRC (equation 5.2-2).

$$\tau = \sigma_n \tan\left(JMC \cdot JRC \cdot log_{10}\left(\frac{JCS}{\sigma_n}\right) + \varphi_r\right), \qquad 5.2\text{-}2$$

Where joint matching coefficient JMC ≥ 0.3
(Zhao, 1997b)

The JMC parameter, if valid, should create a discrepancy between tilt test obtained values of JRC and profiling values of JRC, with the tilt test results producing lower JRC values. This matches the current data obtained during laboratory work (Table 9).

Table 9: The ratio of profile JRC to tilt test JRC, which can be interpreted as joint matching JMC.

Sample	Ratio (JMC?)
Diorite-1	0.46
Diorite-3	0.57
Diorite-2	0.64
Ore-2	0.59
Ore-1	0.72

Pressure paper tests for JMC comparison

An additional exercise was undertaken to get more information on joint matching behaviour. Two pressure paper tests were performed on one of the tested diorite samples (labelled Diorite-2 or PR2) in connection with the KARMO project at Aalto University (Kopaly & Uotinen, 2015).

A pressure paper test is designed to show the area of contact between two samples by applying pressure on the contact surface. The ink within the paper used in the test gets triggered when enough pressure is put on it, colouring the pressurized area red. Areas of non-contact are assumed not to trigger the paper, leaving the corresponding area white. The proportion of coloured area out of the whole sample area is presumed to estimate the JMC parameter.

The used paper was Fujifilm Prescale LLLW 0.2-0.6 MPa and Fujifilm Prescale LLW 0.5-2.5 MPa. It was placed between the sample halves and a normal stress of 0-1.0 MPa was applied over 120 seconds and kept at 1.0 MPa for another 120 seconds. (Kopaly & Uotinen, 2015).

A post-test photograph of two papers of different sensitivity is shown in Figure 5-8. The total sample area can be estimated from the shape of the partially triggered area. The results show a matching surface area of about 60 % (LLW paper) and 90 % (LLLW paper), both of which are realistic considering the current data. LLW-obtained matching is closer to the coefficient obtained using profile comparison and tilt test JRC values, which were 5.3 and 8 respectively, giving JMC = 0.66. Further investigation using pressure paper can be of value in understanding the effect of joint matching on joint roughness mechanics.

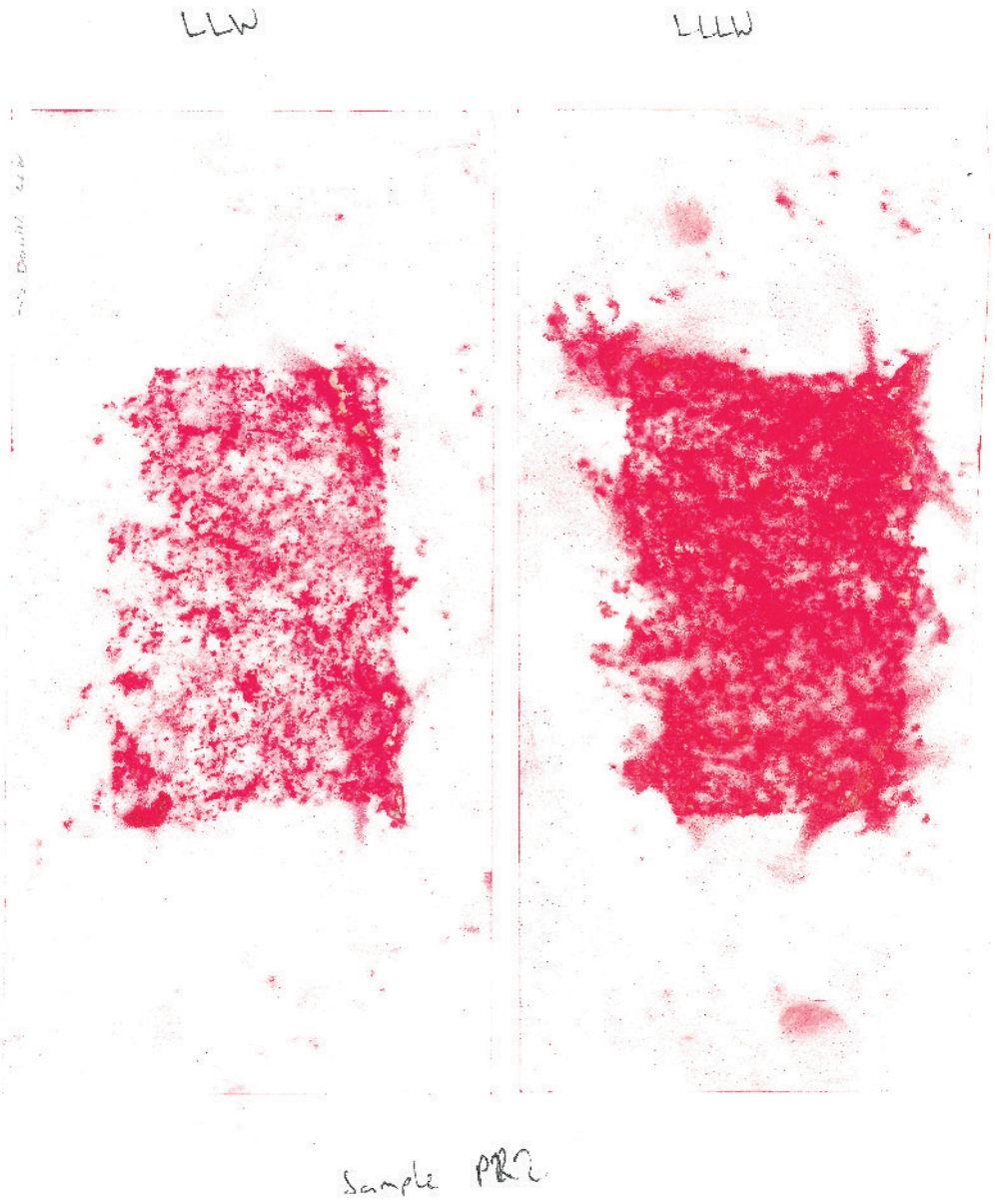

Figure 5-8: Pressure paper results (Kopaly & Uotinen, 2015). Red areas represent triggered contact points.

5.3 ISSUES OF RESULT VARIABILITY

As can be seen in Figure 4-6 and Figure 4-5, the results are variable between samples of the same type, especially for Mohr-Coulomb fits. Biased sample selection, discussed above, can have an effect on result variability, but cannot explain it completely (and the effect may be negative). As can be seen in the figures, there is a fairly strong correlation between BB parameters (mainly JRC) and MC/SB results.

Joint roughness is assumed to be the main varying parameter, as variability of ϕ_r is quite limited, and JCS variability would need to be logarithmic to have significant effects on BB results. Thus any further research needs to start with profiling JRC at relevant locations and recording the variability e.g. using histograms. Using this data, relevant samples can be selected and used to obtain the necessary parameters for either model.

5.4 SIMULATION AND PREDICTION ISSUES

The main issue of any scientific model is that it is an inevitable simplification of the phenomenon it attempts to describe. Whether or not this is an actual problem for design depends on whether model's simplifications are somehow significant design-wise.

The simplification of the Mohr-Coulomb model is obvious: it is merely a linear fit of known data, despite knowledge that discontinuity and rock mass stability behaviour is not linear. However, as long as natural variability of rock behaviour is significantly higher than the error created by this simplification, the model can be seen as valid for design. The natural variability of course forces the use of higher safety factors than when working with isotropic building materials such as concrete. This is, however, an issue of data gathering economics: how much data gathering can be justified compared to the additional accuracy gained?

A greater issue for the MC model is that it is based on small-scale laboratory test which are not simple to scale to design dimensions of in-situ block sizes. Small-scale tests also produce disproportionately high variability in resulting strength estimates. Due to this and the fact that no single clear scaling method exists, (shear box) laboratory test results should currently only be used as a starting point for back-calculations, or for comparison with literature values.

The Barton-Bandis model is physically coherent in attempting to take into account the different components of the shear strength of joints. This does not automatically mean that it is completely correct. For example, it has been purported to underestimated shear strength at very high stresses. It is still likely closer to in-situ behaviour than MC. With the current, albeit limited, amount of data back-calculations did not show a need to change the original parameters obtained by laboratory and in-situ tests.

Partly due to sheer luck, the lowest unscaled MC results based on shear box tests in this study also came very close to the behaviour given by the BB model. This result is not completely unexpected: with high variability results at small scale, the parameters will scale negatively, i.e. become lower with greater dimensions. Thus the scaled parameters can be expected to be below average.

Diorite failure simulation showed the produced BB and MC parameters to give a safety factor close to one and suspect, but not failed simulation gave a safety factor of about 1.5 for a continuous joint and a little under one for a joint that is likely discontinuous, meaning a cohesion factor is at play. This is a promising result as it conforms to the proposed failure models.

Failures in ore, on the other hand, resulted in a back-calculated safety factor of 0.1 to 0.3, much lower than can be expected for failures which were not instant post-blast. However, these had a height of merely several meters, and a quick glance at the failure surfaces shows that they involved not only joints, but failure of intact rock, meaning that an intact rock strength (cohesion) factor should have been included in the back-calculations to obtain the real safety factor produced by the model. No clear suspect areas were found for simulation.

Joint continuity, however, is difficult to predict without extensive further research into the variability of such continuity. To be on the safe side, it may be better to assume continuous joints when evaluating possible instabilities. On the other hand, this may lead to overly conservative estimates, as a disproportional amount of natural joint sets include discontinuous joints and/or a small block size, both of which add strength and require more complex simulation.

5.5 COMPARISON OF RESOURCES AND USEFULNESS FOR EACH METHOD

Both methods require certain amounts of time, trained personnel, testing equipment and monetary resources. These cannot be known exactly without specific understanding of the project, and they depend on each other. However, some comparisons and general estimates are given below.

The time it takes to get laboratory and in-situ test results is dependent on several factors. One of these is whether or not laboratory equipment is at the researchers' disposal on-site, and how far it is if not. The farther away the laboratory the more temporal and monetary resources will be needed to get the necessary samples there. Besides this, most outside laboratories have a schedule of their own, so waiting time needs to be budgeted as well as monetary costs.

The Barton-Bandis method needs less samples of the joint surface to achieve the same result variability. However, it needs information of the basic friction angle (obtained from drill cores, often readily available) and uniaxial compressive strength of the rock (which is usually already known due to tests done for rock mass property determination, or a literature value is used).

Overall it is more likely that determining Barton-Bandis parameters needs less work in obtaining extra samples. It also needs less complex and costly equipment (a Schmidt hammer, a tilt table and possibly a profilometer), thus a makeshift laboratory is easier to set up on-site, saving in both time and money.

The sample extraction time is the same for both MC (shear box) and BB (tilt table) tests. However, shear box tests require further sample preparation (casting), which can incur up to two days extra waiting time when concrete is used for the casting. The actual shear box test can take up to several hours, while a tilt table test generally takes less than half an hour after determining the possible range of tilt table slope angles at joint failure. Additionally, shear box tests require more understanding of the operated machinery and test design than the training required for use of a tilt table and Schmidt hammer. The resulting MC data is also more laborious to interpret properly.

Having obtained test results and the possible range of each model's parameters, further research possibilities at local instabilities are very different. The only information that can be gained to augment the MC model is intuitive comparison of seen joint types to tested samples by an experienced designer. For BB, on other hand, it is possible to gain additional understanding by profiling any joint of interest using conventional methods such as a brush gage profilometer or a straightedge and ruler. Profiles can then be compared to joint samples tested earlier. A future possibility is to use photogrammetry or laser scanning methods for automatic joint profiling.

One issue for the BB model is that it is not available for direct use in all simulation software, while MC parameters are an industry standard. However, it is fairly simple and requires little extra work to fit a line to the generated BB curve for the used stress levels.

Overall it is difficult to evaluate the overall accuracy of either method. Shear box results are more variable and more difficult to interpret than the obtained Barton-Bandis parameters. However, both selected parameters were shown not to be completely wrong; i.e. they produced the expected safety factors; above or below one depending on failed and not failed status. Further data gathering would be needed for a proper statistical analysis.

5.6 SUGGESTIONS FOR FUTURE FAILURE SIMULATIONS AT SIILINJÄRVI

Based on the results generated in this study, it is recommended that a more extensive and systematic gathering of Barton-Bandis parameters is undertaken at the mine site. Necessary research is described below. It needs to be noted that the Barton-Bandis model was designed to incorporate

softening filling, so it needs to be used with caution when considering the slippery chlorite filling in the ore.

The basic friction angle of each rock type should be obtained by using existing drill cores. The cores should be sawn to a standardized length, and any cores with visible drill ridges should be discarded. Each core assembly must be tested multiple times, turning each core in turn between tests. Two core tilt tests are the currently recommended setup. Rocks known to be anisotropic may need to be tested in various directions in respect to the anisotropy.

For the compressive strength of rocks, old test data can be analysed to determine variability and its causes. If that is insufficient, new tests must be carried out which record the test direction in respect to any anisotropy in the rock. If possible, nearby or even same sample should be tested using a well-calibrated Schmidt hammer to obtain a correlation of the Schmidt hammer index and compressive strength.

Schmidt hammer tests need to be carried out on large blocks as well as on in-situ samples. Laboratory samples may also be used to compare in-situ and laboratory (matrix saturation) results. Any joint filling in the samples must be recorded in connection with these tests so that valid comparisons are possible. The correlation of calibrated compressive strength values should be used to gain joint compressive strength values from the Schmidt rebound value, as merely comparing rebound values only gives an approximation of the strength. The rebound values are, however, necessary for obtaining the residual friction angles.

Obtaining the joint roughness coefficient and understanding its variability is the most challenging part of future research, and some of the issues concerning it are highlighted below in section 6: Areas of further research. As the only relatively reliable method of obtaining the JRC parameter without having to consider effects of joint matching is tilting of geometrically simple samples, it is highly recommended to obtain a large series of joint samples using as large of a core diameter as feasible, preferably 100 mm or larger. Such samples can also be used for shear box testing if necessary. The same samples should be profiled prior to testing using both methods suggested by Barton, and the correlation between each result should be analysed so that in the future simple profiling would be enough to obtain the JRC parameter.

On the other hand, all possible failures should be documented for simulation to check the obtained parameters for validity. Documentation should include the following information:

- Failure date
- Failure location
- Local weather records for the past two weeks or more
- Rock and joint type(s) involved
- Photographs of post-failure joint surfaces
- Joint surface orientations (dip and direction)
- An evaluation of possible joint discontinuity which could have created a cohesion factor
- A description of the failure and other necessary notes
- Pre-failure photographs, if possible
- A systematic joint profiling, if possible

Similar documentation should be done for any suspected joint-dominated failure areas, such as wedges. The current main areas of interest for joint shearing simulations are ones with failures dominated by sliding on joint surfaces. These include diorite areas with continuous planar jointing and ore areas with chlorite-covered jointing.

Using this documentation the known and suspected failures should be simulated in relevant software. If the parameters are valid, the models should produce a safety factor of less than one for known failures. For suspect areas which have remained stable for a considerable length of time, the produced factor of safety should be greater than one. Remember to account for water flow, ice wedging and other weather-related issues when simulating, as well as possible cohesion due to discontinuous joints!

Use of the process introduced in Figure 2-9 should be continued to determine the necessity of simulation for each suspected failure risk. Since less work is now required to simulate the types of failures discussed in this thesis, the decision to simulate can be taken more often than before. Simulation can be carried out using Swedge software for wedges and spreadsheet calculations for plane failures. Use of 3DEC is not recommended for most cases, as building a single model can be unnecessarily resource-consuming.

Input of correct parameters for the simulation is essential. For the Barton-Bandis model the parameters provided in this thesis can be used as a starting point. It is however important to at least visually check the correspondence of joint roughness in the discontinuity of interest to the tested discontinuities of this study. Even more importantly, correct input of the discontinuity and wall parameters – dip and dip direction – is necessary for a useful result. For joints which are suspected to be discontinuous it is left up to the designer to assess how conservative the simulations are.

6 AREAS OF FURTHER RESEARCH

The suggestions specific for Siilinjärvi in section 5.6 can be generalised for further research at other sites. Other findings of this study prompt more suggestions for further general research on the methods and theory introduced in this work. These are discussed below.

6.1 CORE TILT TESTS

According to Barton, using a three core tilt test is never recommended due to a wedging effect that would bias the obtained results (Barton, 2013; Barton, 2015). The relevance and size of this effect remains unclear, thus a further comparative investigation in footsteps of Ruiz & Li (2014) should be carried out to determine the necessity of using a two core test when a three core test is simpler to carry out. Sandblasting of the tested surfaces should also be considered and result between blasted and unblasted surfaces can be compared.

6.2 INVESTIGATIONS IN JOINT ROUGHNESS

The joint roughness parameter JRC of the BB model is defined quite simply as any shear strength that a sample generates above the basic or residual friction of the rock or joint. This parameter is easily obtained using tilt tests of joint surfaces; however, this requires good sampling of the relevant joints. Two ways to estimate the JRC parameter instead have been developed, which are profile comparison and profile height-to-length (a/L) measurement.

These profiling methods are simple to perform both on laboratory samples and in-situ. However their correlation to the actual JRC parameter seems to be affected by the extent to which the joint halves match. This matching cannot be measured using only one side of the sample, thus for each joint type which is relevant, the correlation coefficient between the profiled and actual JRC – also known as the joint matching coefficient JMC – should be measured, as well as the variability of this coefficient.

Another issue arises for the a/L method specifically: using a simple thought experiment (Figure 5-5) it is shown that likely the same a/L results can be obtained for very different actual JRC values. The correlation between the a/L method result and actual JRC is likely specific to rock and joint type. Thus this correlation should be obtained and the formula (equation 5.2-1) used should be corrected separately for each joint or rock type.

6.3 ESTIMATIONS OF JOINT CONTINUITY

When simulating failure along joint planes, it is assumed that joints are continuous and cohesion is non-existent. This is a conservative and safe assumption. However, it may be wrong as joints can be discontinuous and direct rock contact may exist, essentially adding shear strength through a cohesion factor as shear strength of the actual rock mass. Affordable methods to investigate continuity of joints should be developed and tested extensively to increase simulaton accuracy and lower expenses.

6.4 SCALING OF SMALL-SCALE LABORATORY TEST RESULTS

Though the general theory of scaling results of small samples to in-situ block size is well known, the actual scaling factors vary due to a variety of factors. Ways of scaling the small-scale laboratory tests used currently, such as shear box tests, is one path that should be undertaken. Further research is needed to determine if after plotting small-scale variability to some sort of statistical distribution, the distribution could be used to determine a sort of convergence curve, where the shear strength would converge from the small-scale variability to the basic friction of the rock at large scale.

Another path is finding a way of testing large-scale specimens at affordable costs. This may be possible by using 3D photogrammetry methods to produce 3D models. These models can then be used for numerical simulations or for creating scaled physical copies of the joint using brittle, rock-like material such as concrete.

6.5 TAKING JOINTS INTO ACCOUNT WHEN SIMULATING ROCK MASSES

When simulating rock mass stability, joints are often input as a weakening parameter of the rock mass. However, often failure zones occur through propagation of joint fractures, and further work can be done to understand this mechanism of failure (Suikkanen, 2014). This could likely produce more specific predictions of failure occurrence, likelihood and timing.

7 CONCLUSIONS

The study's objective was to find the most applicable method for rock joint stability analysis, both at the Siilinjärvi case site and in general. While the results are not conclusive, the Barton-Bandis model has shown more promise both in the amount of resources required for obtaining relevant parameters, and for result validity. It is still recommended to settle the matter by gathering a large amount of data for parameter variability analysis, including joint continuity if possible.

Both MC and BB methods can use similar samples for their main parameters. Sample selection and handling, however, needs to be standardized before conducting any further research. Joints need to be selected based on relevancy in respect to the failure modes of interest, and sample extraction and further handling need to be designed so as to minimize sample damage and any need to further modify the sample prior to laboratory testing.

Besides standardization of sample extraction and handling, the laboratory tests also need to be standardized based on the finding presented in this thesis. Sample sizes, test amounts and other factors need to be accounted for.

There are several stark differences between the two models, concerning both the work done to obtain model parameters and the resulting strength estimates. For reliable Mohr-Coulomb results, multiple shear box tests of relevant samples need to be done. For any new joint types or specific failure areas, a new, albeit smaller, test series will be needed. For Barton-Bandis, on the other hand, an extensive series of tests are first needed to determine the less variable parameters of each rock type: the basic friction and compressive strength. Another extensive series will be needed to estimate the variability of joint roughness and the correlation between laboratory-obtained joint roughness and profiling results. The amount of work this requires is in the same ballpark as for the Mohr-Coulomb model. However, data for any specific location is easy to obtain later on with simple in-situ index tests, requiring minimal resources.

Shear box tests produce highly variable results, especially for rough joints. These results need to be scaled to in-situ block size, which is difficult at best. Barton-Bandis parameters vary considerably less and joint roughness has the most effect on strength estimation, making it easier to use. Overall the conclusion of this study is that using Barton-Bandis parameters for joint stability analysis likely creates added value to a project with joint stability risks. This added value is created by reducing the workload and increasing the accuracy of simulating and predicting small-scale failures.

During the study it was noticed that there is a significant discrepancy between laboratory-obtained JRC values and corresponding JRC values obtained using profiling. There is also a high discrepancy between the two profiling methods used. This suggests the need for further research on obtaining these parameters.

8 REFERENCES

ADAM Technology, 2014. *3DM Analyst.* s.l.:s.n.

Atlantic Supply, 2015. *Type N Schmidt Concrete Test Hammer.* [Online]
Available at: https://www.atlanticsupply.com/product_item.asp?id=1849
[Accessed 27 July 2015].

Aydin, A., 2009. ISRM Suggested method for determination of the Schmidt hammer rebound hardness: Revised version. *International Journal of Rock Mechanics & Mining Sciences,* Volume 46, pp. 627-634.

Bahaaddini, M., Hagan, P. C., Mitra, R. & Hebblewhite, B. K., 2014. Scale effect on the shear behaviour of rock joints based on a numerical study. *Engineering Geology,* Volume 181, pp. 212-223.

Bandis, S., Lumsden, A. C. & Barton, N., 1981. Experimental Studies of Scale Effects on the Shear Behaviour of Rock Joints. *International Journal of Rock Mechanics and Mining Sciences & Geomechanics Abstracts,* Volume 18, pp. 1-21.

Barton, N., 1973. Review of a New Shear-Strength Criterion for Rock Joints. *Engineering Geology,* Volume 7, pp. 287-332.

Barton, N., 1981. *Shear Strength Investigations for Surface Mining.* Vancouver, British Columbia, Society of Mining Engineers of AIME, pp. 170-196.

Barton, N., 1982. *Modelling rock joint behavior from in situ block tests: implications for nuclear waste repository design,* Salt Lake City, UT (USA): Terra Tek, Inc..

Barton, N., 1999. *General report concerning some 20th Century lessons and 21st Century challenges in applied rock mechanics, safety and control of the environment.* Leiden, Netherlands, Balkema, pp. 1659-1679.

Barton, N., 2013. *Course: The Q-system in Rock Engineering.* Espoo, s.n.

Barton, N., 2015. *E-mail exchange* [Interview] 2015.

Barton, N. & Bandis, S., 1982. *Effects of Block Size on the Shear Behaviour of Jointed Rock.* Berkeley, California, Society of Mining Engineers of AIME, pp. 739-760.

Barton, N. & Bandis, S., 1990. *Review of predictive capabilities of JRC-JCS model in engineering practice.* Loen, s.n.

Barton, N., n.d. *Estimating Barton-Bandis Input Parameters.* [Online]
Available at: https://www.rocscience.com/help/rocdata/webhelp/rocdata/Estimating_Barton-Bandis_Input_Parameters.htm
[Accessed 19 05 2015].

Barton, N. R. & Choubey, V., 1977. The shear strength of rock joints in theory and practice. *Rock Mech.,* 10(1-2), pp. 1-54.

Castelli, M., Re, F., Scavia, C. & Zaninetti, A., 2001. *Experimental Evaluation of Scale Effects on the Mechanical Behaviour of Rock Joints..* Espoo, Finland, Taylor & Francis, pp. 205-211.

Finnish Meteorological Institute, 2015. *Kuukausitilastot.* [Online]
Available at: http://ilmatieteenlaitos.fi/kuukausitilastot
[Accessed 3 August 2015].

Franklin, J. & Dussealt, M., 1989. *Rock Engineering.* New York: McGraw-Hill.

Hoek, E., 2006. Shear strength of discontinuities. In: *Practical Rock Engineering.* s.l.:s.n., p. 14.

Hoek, E. & Bray, J. W., 1981. *Rock Slope Engineering.* 3rd ed. London: The Institution of Mining and Metallurgy.

Hoek, E., Wood, D. & Shah, S., 1992. *A modified Hoek-Brown failure criterion for jointed rock masses.* Chester, s.n.

Itasca Consulting Group, Inc., 2013. *3DEC 5.00.* s.l.:Itasca International.

Karzulovic, A. & Read, J., 2011. Rock mass model. In: J. Read & P. Stacey, eds. *Guidelines for open pit slope design.* Leiden, Netherlands: CRC Press/Balkema, pp. 83-140.

Kauppinen, H., 1989. *Siilinjärven avolouhoksen seinämäkaltevuuksien laskentaa 1989 varten,* s.l.: s.n.

Kopaly, A. & Uotinen, L., 2015. *KARMO painekalvotestit 13.5.2015,* Espoo: s.n.

Korpi, E., 2012. *Kalliorakojen rasialeikkauskoe (Bachelor's Thesis: Shear Box Test of Rock Joints),* s.l.: s.n.

Kutter, H. & Otto, F., 1990. *Influence of parallel and cross joints on shear behaviour of rock discontinuities.* Loen, Norway, International Society for Rock Mechanics.

Lamberg, M., 2015. *Interview with Pöyry geologist* [Interview] 2015.

Leal-Gomes, M. J. A., 2003. *Some New Essential Questions about Scale Effects on the Mechanics of Rock Mass Joints.* Sandton, South Africa, International Society for Rock Mechanics.

Muralha, J. et al., 2013. ISRM Suggested Method for Laboratory Determination of the Shear Strenght of Rock Joints: Revised Version. *Rock Mechanics and Rock Engineering,* 47(1), pp. 291-302.

Nick Barton & Associates, 2014. *Siilinjaarvi Open Pit Mine Stability Aspects,* s.l.: s.n.

Nick Barton & Associates, 2014. *Siilinjaarvi open pit mine stability aspects: a record of conditions observed, and advice concerning shear strength estimation for input to numerical models (3DEC and FEM/FLAC),* s.l.: Yara Finland.

Reeves, M., n.d. *Laboratory Tests.* [Online]
Available at: http://homepage.usask.ca/~mjr347/prog/geoe118/geoe118.034.html
[Accessed 27 July 2015].

Rocscience Inc., 2015. *Swedge 6.008 64-bit.* Toronto, Ontario, Canada: Rocscience Inc..

Ruiz, J. & Li, C., 2014. *Measurement of the basic friction angle of rock by three different tilt test methods.* Vigo, Spain, Taylor & Francis Group, pp. 261-266.

Suikkanen, J., 2014. *Modeling slope stability utilizing fracture mechanics.* Espoo, Finland: Aalto University.

Szilágyi, K., 2013. *Constitutive modeling of rebound surface hardness of concrete.* [Online]
Available at: http://doktori.bme.hu/bme_palyazat/2012/hallgato/honlap/szilagyi_katalin_en.htm
[Accessed 27 July 2015].

Ueng, T.-S., Jou, Y.-J. & Peng, I.-H., 2010. Scale Effect on Shear Strength of Computer-Aided-Manufactured Joints. *Journal of Geoengineering,* 5(2), pp. 29-37.

Ulusay, R. & Hudson, J. A., 2012. Suggested Methods for Rock Failure Criteria: General Introduction. *Rock Mechanics and Rock Engineering,* Issue 45, p. 971.

Weber, 2015. *weber.vetonit JB 1000/3.* [Online]
Available at: http://www.e-weber.fi/tekniset-laastit/tuotteet/juotos-ja-saumausbetonit/webervetonit-jb-10003.html
[Accessed 24 March 2015].

Wesseloo, J. & Read, J., 2011. Acceptance criteria. In: J. Read & P. Stacey, eds. *Guidelines for open pit slope design.* Leiden, Netherlands: CRC Press/Balkema, pp. 221-236.

Yara, 2013. *Siilinjärvi Phosphate Mine – fourth decade ongoing.* [Online]
Available at: http://fem.lappi.fi/c/document_library/get_file?folderId=1405164&name=DLFE-20769.pdf
[Accessed 6 2015].

Zhao, J., 1997a. Joint Durface Matching and Shear Strength Part A: Joint Matching Coefficient (JMC). *Int. J. Rock Mech. Min. Sci,* 34(2), pp. 173-178.

Zhao, J., 1997b. Joint Surface Matching and Shear Strength Part B: JRC-JMC Shear Strength Criterion. *Int. J. Rock Mech. Min. Sci.,* 34(2), pp. 179-185.